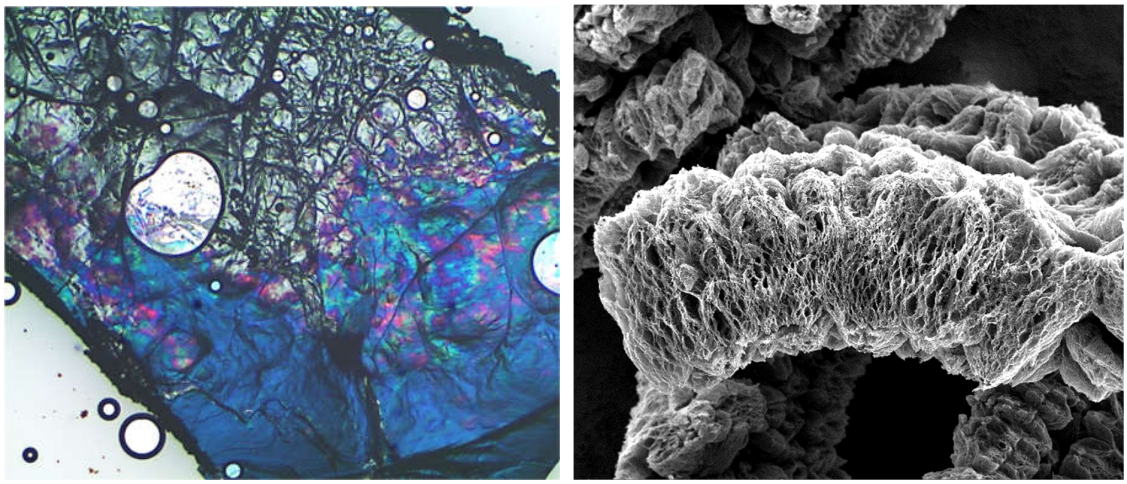

Intercalation and exfoliation of graphite

- For a route to scalable production of conductive inks for printed electronics

Master's thesis in Materials and Interface Chemistry

PATRIK KARLSSON

Department of Chemistry and Chemical Engineering,
CHALMERS UNIVERSITY OF TECHNOLOGY
Gothenburg, Sweden 2016

MASTER'S THESIS 2016

Intercalation and exfoliation of graphite
- For a route to scalable production of conductive inks for printed electronics

PATRIK KARLSSON

CHALMERS
UNIVERSITY OF TECHNOLOGY

Department of Chemistry and Chemical Engineering
Division of Applied Surface Chemistry
Chalmers University of Technology
Gothenburg, Sweden 2016

Intercalation and exfoliation of graphite
-For a route to scalable production of conductive inks for printed electronics.

Patrik Karlsson

Supervisors: Prof. Bert de With, Dr. Heiner Friedrich, Dr. Maurizio Villani at Materials and Interface Chemistry, Eindhoven University of Technology and Prof. Hanna Härelind at Applied Surface Chemistry, Chalmers University of Technology.

Examiner: Prof. Hanna Härelind, Applied Surface Chemistry, Chalmers University of Technology.

Master's Thesis 2016

Department of Chemistry and Chemical Engineering

Division of Applied Surface Chemistry

Chalmers University of Technology

SE-412 96 Gothenburg

Cover: Left: A flake of highly oriented pyrolytic graphite undergoing color changes as the intercalation reaction using sulfuric acid and ammonium persulfate progresses. Right: SEM image of sulfuric acid-persulfate expanded graphite flakes.

Gothenburg, Sweden 2016

Intercalation and exfoliation of graphite
- For a route to scalable production of conductive inks for printed electronics

Patrik Karlsson
Department of Chemistry and Chemical Engineering
Chalmers University of Technology

Abstract

The ability to print environmentally friendly, lightweight, foldable conductors with the performance of rigid-based electronics would open up for a new area of applications. Research regarding ink formulations containing graphene has shown promising results for this application. Exfoliation of graphite is the first reported top-down method that produced single or few layered graphene. However, an exfoliation method that has a good yield, can maintain the integrity of the sheets, control the thickness of the material and be produced in an economically viable scalable production method is still not available. One approach to improve the method is by creating a graphite intercalation compound before the sheets are separated. Further details on the formation and properties of the graphite intercalation compounds concerning the characteristics mentioned above, is needed.

Due to sulfuric acids ability to form a stable intercalation compound with graphite at ambient conditions it was chosen as the study subject. The aim of this work it to study properties and formation of sulfuric acid graphite intercalation compound in a model system, using optical microscopy and Raman spectroscopy to characterize the reaction in real time. Additionally, the intercalation compound was confirmed by XRD and experiments concerning exfoliation and expansion of the material was performed and characterized with SEM and EDX.

The results sheds light on intercalation dynamics and how to control it. Keeping the oxidant concentration constant and increasing the concentration of sulfuric acid by adding Oleum had a strong effect on the reaction speed, from visually observing a stage-1 compound within 1 hour using 95-98% sulfuric acid to within 1 minute using a 50/50 mixture of Oleum and 95-98% sulfuric acid. Optical microscopy shows that the sulfuric acid graphite intercalation reaction manifests as a curvature front moving over the surface, propagating from the edges to the center followed by a second curvature front moving in the same way. This indicates that the major part of intercalant enters from the edges, along the planes, into the graphite crystal. This makes the flake size a critical factor when performing the reaction. Raman spectroscopic data indicates that surface intercalation is faster than bulk intercalation. A relation for the time dependency of the expansion (μm/s) was established.

The ability to limit the staging is relevant for creating a material with a defined platelet thickness as well as for scalability, when a process which is not sensitive to increase in reaction time is wanted. It is shown that by diluting the sulfuric acid in the reactant composition, the staging was limited to the formation of a stable stage-2 compound.

It is shown that the degree of expansion and delamination can be controlled by tuning the concentration of oxidant, where the most expanded graphite material was found to be produced using a ($(NH_4)_2S_2O_8$ [g])/(graphite [mg]) ratio of 0.005-0.01 and a concentration of $(NH_4)_2S_2O_8$ at 0.877M. De-intercalation experiments show that higher stagnings of the sulfuric acid GIC is stable in water, and hence even might pose a problem when removal of all intercalants is wanted.

Keywords: intercalation, sulfuric acid intercalation compound, graphene, graphite, GIC

Acknowledgements

I want to thank Hanna Härelind, my examiner at Chalmers, for letting me do the project abroad and for your positive attitude and help during my whole project. I also want to thank my supervisors at Eindhoven University of Technology; Heiner Friedrich and Bert de With for accepting my application, giving me the opportunity to write my thesis at the SMG group and for all the valuable discussions we had. Special thanks to Maurizio Villani for coaching me during the project and for helping me with the XRD measurements and introducing me to the optical microscope. Further thanks to my room mates Zino Leijten and Joe Patterson for your help and good talks. Thanks to Kirill Arapov for exchange of ideas and for help with the SEM and microwave expansion and to Jos Laven for introducing me to the Raman spectroscope. Gratitude towards the whole SMG group, and to those I acquainted in SPC group, for your help and for being so nice to me. Thanks to all my friends and especially Karen for your love and support. Thanks to ÅForsk for the financial support. And finally thanks to Netherlands for being such a welcoming country and home of many good beer breweries.

Patrik Karlsson, Gothenburg, 2016

Table of contents

Nomenclature

Intercalant(s)..... A specie (an atom or molecule, for example sulfate ions) that is inserted between layers in layered material.

Intercalation..... The insertion of intercalants between layers in a layered material.

De-intercalation ..... The removal of intercalants in a layered material, see intercalation.

Staging ..... The number of sheets next to each other in an intercalated material, the lowest achievable staging is 1.

Exfoliation..... The complete separation of sheets in a layered material.

Chemical substances and corresponding formulas

Sulfuric acid – H_2SO_4

Oleum – *Sulfuric acid* with dissolved sulfur trioxide (SO_3), eliminating the presence of water.

Ammonium persulfate/Ammonium peroxydisulfate – $(NH_4)_2S_2O_8$

Abbreviations

LPE – Liquid phase exfoliation

GIC – Graphite intercalation compound

HOPG – Highly oriented pyrolytic graphite

XRD – X-ray diffraction

SEM – Scanning Electron Microscope

EDX – Energy dispersive X-ray spectroscopy

OM – Optical Microscopy

1. Introduction

In the field of printed electronics, the ability to print environmentally friendly, lightweight, foldable conductors with the performance of rigid-based platforms would open up for a new area of applications. It would make it possible to integrate devices such as solar cells, sensors (temperature, gas, etc.), screens, memory storage and network communication into flexible consumer products [1]. A material that combines the properties needed to achieve these goals, such as flexibility, low electrical resistivity, durability and ease of recycling with a low-cost mass production method is not yet available. However, research regarding the material graphene has shown promising results for all of the properties mentioned [2].

Before mass production of graphene devices can be realized, a large scale cost effective production method must be established. One of the top-down production methods starts with bulk graphite and then tries to separate the graphitic layers (exfoliation) in a solvent to acquire graphene or few-layered graphite [3]. This process, referred to as liquid phase exfoliation (LPE) of graphite, shows promise in producing a material that can be used in for example inks, coatings and batteries [2]. To enable the exfoliation some input of energy to the graphite lattice is required [3]. Applicable approaches are sonication, shear mixing or electrolysis, with or without assistance of organic solvents, surfactants and/or ionic liquids. The main issue with the energy input to the lattice, such as the sonication method, is its low yield of graphene because sheets break into smaller sheets, defects are induced and it is hard to control the sheet thickness.

One of the graphite LPE methods uses a route where the graphite is first being subjected to insertion of atoms or molecules (intercalants) between the planes (intercalation) in the graphite to acquire a graphite intercalation compound (GIC) [4]. Intercalation of graphite increases the distance between the graphite layers which weakens the van der Waals attraction between the layers and decreases the energy input needed for exfoliation, and hence possibly also maintains the integrity of the graphene sheets [5]. Although, the driving force for the GIC formation relies on electron transfer to or from the graphene layers in the graphite structure, which itself can induce defects. Interestingly *Dimiev et al. (2012)* reported a reversible formation of a sulfuric acid GIC, using ammonium persulfate [6]. However, the mechanism and degree of reversibility is not clear and it has been questioned by *Eigler (2015)* [7].

The main reason that the graphite intercalation compound-liquid phase exfoliation (GIC-LPE) method is not used extensively for graphene production today is because most GICs tends to degrade in contact with air/moisture and needs controlled ambient conditions during the processing. For example, the potassium GIC is pyrophoric in contact with air. To enable a scalable GIC-LPE method, further details on the formation and properties of GICs that are temporarily stable under ambient conditions is needed [2]. Due to sulfuric acid being a dehydrating agent and its ability to form an intercalation compound with graphite it is a suitable starting point for studying GICs.

The sulfuric acid GIC formation is conducted in a liquid environment and in strong sulfuric acid which defines the criteria of the reaction setup. Another aspect in the choice of method is that the intercalation formation gives rise to colors in the visible spectra. The material is also active in the Raman spectra which enables the degree of intercalation to be monitored. The characterization properties of sulfuric acid GIC in combination with the strong corrosive environment present made the choice of method to be performing reactions on glass slides with cover glass, while characterizing the reaction in real time using optical microscopy and Raman spectroscopy. Additionally, the intercalation compound is to be confirmed by XRD and experiments concerning exfoliation and expansion of the material is to be characterized with SEM and EDX as well.

1.1. Aim

The aim of this work is to investigate the dynamics of sulfuric acid GIC formation to enable industrially scalable production of exfoliated graphite for use in conductive inks. To study the process a model system was chosen, consisting of cut flakes of highly oriented pyrolytic graphite and naturally flaked graphite, systematically reacted with various sulfuric acid and persulfate reactant solutions while monitored and characterized with optical microscopy and Raman spectroscopy. The results forms the base for a discussion regarding kinetics, stability and formation of sulfuric acid graphite intercalation compounds in relation to a scalable process.

2. Theory

Graphene and graphite

Graphene is a two dimensional (2D) crystal consisting of sp^2 hybridized carbon atoms with delocalized pi-electrons. Due to the material being 2D and due to the presence of van der Waals forces between the sheets, it is stackable. This is why graphene is most commonly found in the form of graphite in nature. The natural graphite can be bought from mining companies in the form of chunks of graphite crystals, and material can then be treated with the proper equipment to form the specimen needed for the application. There are also standardized pre-treated graphite material, one of them is flaked graphite, where the graphite has been milled and then sorted according to flake size. Apart from the natural sources of graphite there is synthetically grown crystals. One such material where the crystal growth has been carefully controlled is highly oriented pyrolytic graphite.

Graphene as a precursor material for conductive inks

Graphene's ability to re-stack makes the material interesting in a conductive ink formulation for printing applications; the idea is that when an ink formulation with dispersed graphene sheets are printed the graphene sheets can arrange to overlap each other to create a tiled and conductive film. Better conductivity is achieved when the graphene sheets are large and the total number of sheet overlaps are few, compared to having smaller sheets and a lot of overlaps.
The fact that the material is carbon makes recycling by burning easier and more environmental friendly than for metal based inks. Graphene has also shown to withstand mechanical deformation, such as folding without breaking. The combination of all the properties mentioned above makes the graphene material highly interesting and it is believed that it will have a major impact in technological advancements.

2.1. Intercalation

The insertion of atoms or molecules (intercalants) between the planes in graphite is referred to as intercalation and the formed material is referred to as a graphite intercalated compound (GIC). The intercalation increases the distance between the layers in the graphite, for example the distance between the layers in pristine graphite is typically 0.34 nm while in a potassium-GIC the sheet distance has been measured to about 0.53 nm (KC_8) [4]. Because of the increased distance between the graphite layers in the GIC the van der Waals attraction between the layers are weakened, and thus the layers can be more easily separated to acquire the desired graphene [5]. The number of layers that are separated by an intercalant layer is defined as staging. A fully intercalated graphite will be a stage 1 GIC, as explained in *Figure 1*.

The intercalation process and the GIC has been shown to be sensitive to the presence of water and air, which induces problems when handling the material. For example, the potassium-GIC is pyrophoric. However there has been recent advancements showing that for example FeCl3-GIC is stable in air [8]. There has also been reported a reversible formation of a H_2SO_4-GIC at room temperature in sulfuric acid under nitrogen [6]. Aspects of the intercalation mechanism still needs to be clarified as well as how the GIC compound interact with different solvents [2]. This knowledge is crucial for achieving a scalable GIC LPE process.

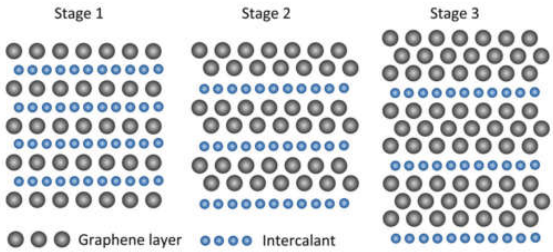

Figure 1. Illustrating the three lowest stagings in a graphite intercalated compound [2].

Sulfuric acid GIC formation

The oxidation formation of sulfuric acid GIC has been described by [9] as follows:

$$C_{24n} + m\,H_2SO_4 \underset{\text{Deintercalation}}{\overset{\text{Intercalation}}{\rightleftharpoons}} C^{+}_{24n}\cdot HSO^{-}_{4}\cdot(H_2SO_4)_{m-1} + H^{+} + e^{-} \quad (1)$$

Equation 1. Showing the reaction between graphite and sulfuric acid, releasing an electron and a hydrogen ion.

The removal of electrons is the driving force for the reaction and the limiting factor is the diffusion of sulfuric acid into the graphite. Depending on what oxidant is used, there are catalysts that speeds up the reaction mechanism, for example silver (I) ions creates a more reactive complex than persulfate ions.

Through electrochemical set-ups the critical electrochemical formation potentials for the different staging has been determined.

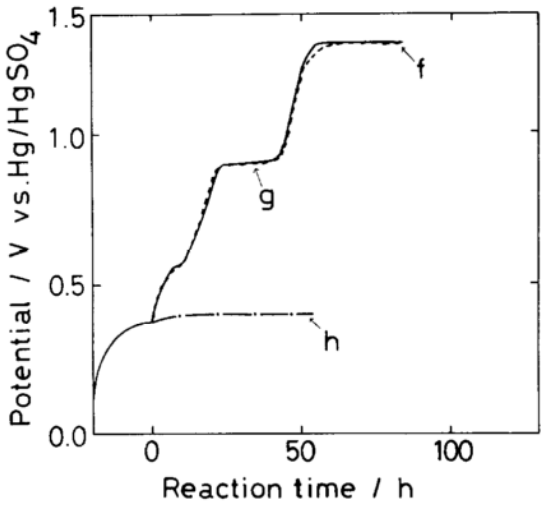

Figure 2. Curves of potential of graphite versus reaction time in 18M H_2SO_4 by chemical oxidation with potassium permanganate [10].

As seen in *Figure* 2 the intercalation strictly follows an order from graphite to higher staging; 0.5V: stage 3 formation; 0.6V: stage 3 fully formed and stage 2 starts to form; 0.9V: stage 2 fully formed and stage 1 starts to form; 1.4V: stage 1 fully formed. The degree of intercalation and hence the potential of the graphite; is determined by the equilibrium potential which is given by Nernst equation, Equation 2.

$\Delta G = nFE_{cell}$, where $E_{cell} = E_{red} - E_{ox}$

Equation 2. Nernst equation.

There's two sides of the reaction; the oxidation potential and the reduction potential. Each staging has a different reduction potential (*Figure 2*) and depending on which oxidation potential is supplied, different staging will be acquired.

The reduction potential can be derived from *Equation 2* and calculated by entering the chemical activities. Looking at *Equation 1*, it can be seen that the reduction potential expression will be dependent on the concentration of sulfuric acid. However measuring the reduction potential directly is also possible, which has been done at different sulfuric acid concentrations by [10] according to:

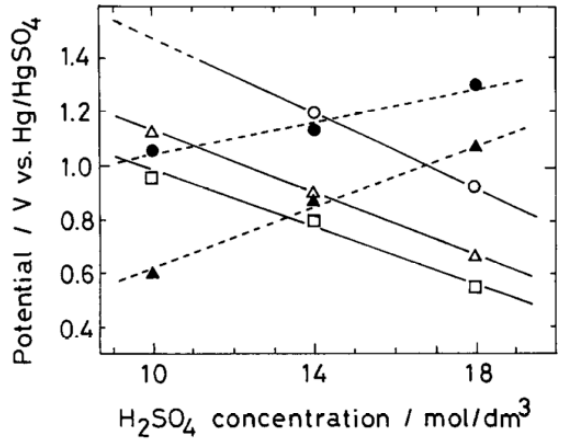

Figure 3. Threshold potentials for stage 1 (○), 2 (△) and 3 (□) sulfuric acid-GICs and upper limits of chemical oxidation potential by permanganate (■) and nitric acid (▲) as a function of sulfuric acid molarity [10].

For the sulfuric acid intercalation compound, a simple way to limit the degree of intercalation is according to *Figure 3* to lower the concentration of sulfuric acid.

The oxidation potential is directly dependent on the activity of the oxidizing specie.

Chemical oxidation

Several oxidizers can be used to provide oxidation potential for the reaction, such as nitric acid and hydrogen peroxide [10]. Another chemical that also has been used for sulfuric acid GIC formation recently is peroxydisulfate [11]. The oxidant has an oxidation potential of 2.01V which is one of the highest electro potentials found in a common oxidizing chemical, however the oxidant has comparatively slower kinetics [12]. The following two step oxidation mechanism has been suggested for the oxidation reaction:

$$S_2O_8^{2-} + M^{n+} \rightarrow SO_4^{2-} + SO_4^{-}\cdot + M^{(n+1)+} \quad (1)$$

$$SO_4^{-}\cdot + M^{n+} \rightarrow SO_4^{2-} + M^{(n+1)+} \quad (2)$$

Equation 3. Proposed peroxydisulfate oxidizing mechanism [12].

The peroxydisulfate decomposes in aqueous solutions [13]. The decomposition mechanism is different depending on the environment:

Reactions at different pH:

Neutral (pH 3 to 7)

$$S_2O_8^{-2} + H_2O \longrightarrow 2HSO_4^- + 1/2O_2$$

Dilute acid (pH > 0.3; [H+] < 0.5M)

$$S_2O_8^{-2} + 2H_2O \longrightarrow 2HSO_4^- + H_2O_2$$

Strong acid ([H+] > 0.5M)

$$S_2O_8^{-2} + H_2O \xrightarrow{H^+} HSO_4^- + HSO_5^-$$

Equation 4. Decomposition mechanism of peroxydisulfate in neutral, dilute acidic and strong acidic conditions [14].

To ensure a constant oxidation potential and a predictable system a low water content is therefore desirable, which has been realized in the model system.

2.2. De-intercalation

The lower stages of the sulfuric acid GIC is temporarily stable as long as the chemical oxidation potential, *Figure 3*, is supplied. When environmental changes that lowers the oxidation potential (dilution of the acid, depletion of the oxidant) happens, de-intercalation follows. The de-intercalation has been found not to proceed in the same ordered fashion as the intercalation does. During the de-intercalation a mixture of stagings are present in the crystal, up to 4 different stagings might be present at the same time:

Table 1. The decomposition of sulfuric acid GIC and the observed color and measured stagings [9].

Time (week)	Color	Observed stage numbers (by X-ray diffraction)
1	Dark blue	1s
2	Blue	1s + 2s
3	Blue	1s + 2s
4	Light green blue	1s + 2s
5	Gray blue	1s + 2s + 3s
6	Silver gray	1s + 2s + 3s
7	Silver gray	1s + 2s + 3s + 4s
8	Silver gray	1s + 3s + 4s + 5s
9	Silver gray	1s + 3s + 4s + 5s
10	Silver gray	1s + 3s + 4s + 5s
11	Silver gray	1s + 3s + 4s + 5s
12	Silver gray	1s + 3s + 4s + 6s
13	Silver gray	3s + 4s + 6s
14	Silver gray	3s + 4s + 6s
15	Silver gray	Graphite
8 months	Silver gray	Graphite

Overall the sulfuric acid GIC it is sensitive for anything that decreases the oxidation potential of the solution, water and decomposition of oxidant for example.

Color changes for GIC

Due to the oxidation of the graphite flake during the intercalation reaction there's a shift of the Fermi energy [15]. For the sulfuric acid GIC stage 1 has been measured to have a fermi energy level of about 1.25eV and stage 2 to about 0.9eV [16]. The energy level of 1.25eV corresponds to 992nm which is near red in the visible spectra, and 0.9eV corresponds to 1378nm which is in the infrared. The stage-1 compound has been shown to appear blue and the stage-2 to stage-1 transition compound shows a mixture of colors [11]. Thus one way to easily monitor the intercalation process for the highest stagings is through optical microscopy.

2.3. Raman signals for graphite materials

Graphite is Raman active, the signals also varies depending on oxidation and defects, which makes the method suitable for characterization [17], [18]. The spectrum of pristine graphite is shown below *(Figure 4)*.

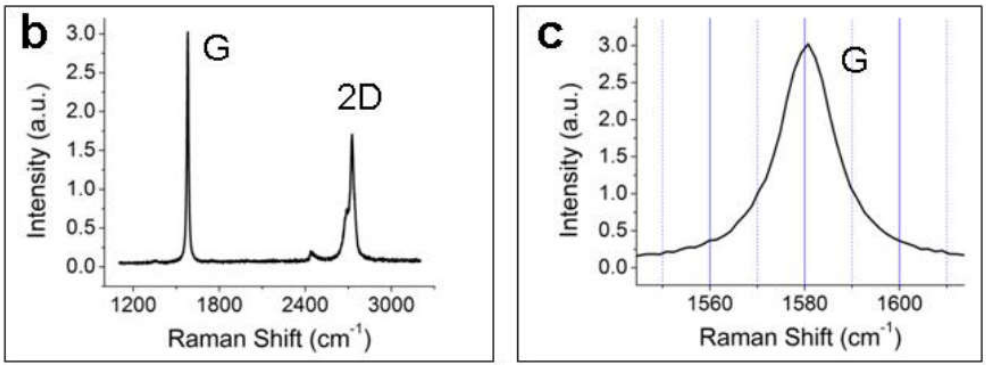

Figure 4 (b, c). The characteristic Raman spectra of pristine graphite, showing the full spectra in (b) and the zoomed in G-peak in (c) [19]**.**

Two distinct peaks (G and 2D) can be identified in *Figure 4*. The G peak origin is believed to be due to sp^2 carbon bond stretch. It has been argued that depending on disorder and defects in the graphite a defect peak, named D also appears at about 1350cm-1 [20]. Grain boundaries and structural defects increases the intensity of this peak. The 2D peak is believed to be a resonance peak of the D peak. The sulfuric acid intercalation compound has been found to have a distinctive Raman spectrum; The D and 2D peaks are dampened out and the G peak is enhanced as illustrated in *Figure 5* below.

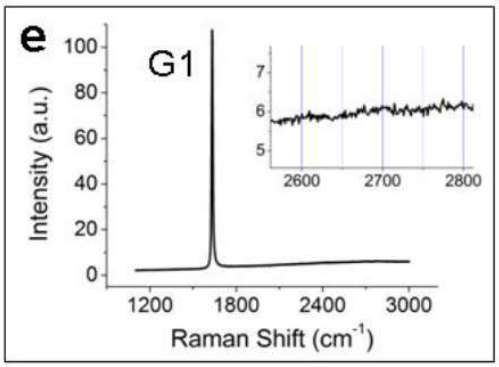

Figure 5. Raman spectra of sulfuric acid GIC, showing the full spectra [21].

Recent publications by *Dimiev et al.* confirms G peak position shift as a function of degree of intercalation staging, shifting the peak higher the lower the staging is. The G peak positions reported are: 1587 (flaked graphite), 1607-1612 (stage >3), 1617-1622 (stage-2) and 1632-1634 (stage-1) [11].

A downside with the Raman analysis technique is that it typically has a probe depth of 1000Å, which basically means near-surface observations of the crystal. The reason for the probe depth is that the material is non-transparent and hence absorbs the light, this makes the need for sufficient heat dissipation of the sample during measurements. Earlier studies has compared the bulk with the surface kinetics with XRD, showing a slower reaction in the inside of the crystal than on the surface [22].

3. Method

The experimental approach consists of four main parts; preparing a model HOPG substrate, reagents, environmental cell for optical microscopy and Raman spectroscopy and finally characterization and analysis. In the following text below, each part is described in more detail.

3.1. Sample preparation

The following types of graphite sources are considered; chunks of natural graphite crystals (Asbury Carbons 2138, Lot: 579605), flaked natural graphite (Alfa Aesar 43319, LOT: J01T026, -10 mesh, 99.9% metals basis) and highly oriented pyrolytic graphite (NT-MDT, HOPG ZYH, 10x10x2mm^3, 3.5-5° mosaic spread, ±0.2 mm thickness dispersion). The samples are illustrated in more detail in *appendix A.1*.

For the quantitative system flaked graphite was chosen, because of its defined bulk properties. The qualitative model system focuses on HOPG, because of its apparent homogeneity, to be able to ensure repeatability and have a predictable system. The natural graphite was only use as a reference and not for any experiments. The size of the prepared samples was matched to the visual observable area of the optical microscope on low magnification (x5), hence the flake size is in the order of 1.2mm to 0.4mm.

The flaked graphite was used as-is. The HOPG samples were prepared by scotch taping a HOPG crystal with thermal tape and then stick it to a glass slide. The glass slide with the attached tape were then put onto a heating plate at 80°C and heated until the HOPG sheet de-adhered (about 3 minutes). Using a pincer, the sheet was put onto another glass slide and then using a scalpel carefully cut into strips of about 1mm in width. Strips were cut into small squares of about 1x1mm. Using the optical microscope (Reichet Polyvar-MET) with low magnification (x5) the crystals were inspected after each scalpel cut to determine which samples to use, based on what appeared to be the most homogenous.

3.2. Reagent preparation

Ammonium persulfate (VWR 0486-100G, APS grade, Lot: S145C456) was added to a vial containing sulfuric acid 95-98% (Sigma-Aldrich 258105-1L, Lot # SZBE3500V) and in some cases also Oleum (Fisher-Scientific 10617761, 20-30% free SO_3, Lot: A0357298). When smaller vials (<10ml) were used the vial was shaken for about 5 minutes, when using larger vials (>10ml) a magnet stirrer is added and the reactant is put to stirring at 400rpm for 10 minutes. The vial was then set to rest for 1 minute to acquire a clear solution. Table of reagents used for the different experiments.

Table 2. The composition of reagents used in the intercalation reactions performed.

Experiment	Sulfuric acid (ml)	Oleum (ml)	Ammonium persulfate (g)	Comments
I	5	-	0.5	
II	4	4	1	
III	4	4	0.9	
IV	5	-	0.625	
V	4	4	1	
VI	5	-	1	
VII	8.3	-	1.8	0.56ml water added
VIII	8.3	-	0.8	0.56ml water added
IX	8.3	-	0.4	0.56ml water added

The reagents in *Table 2* are based on the work on *Dimiev et al.* [6], [11], [23] and variations on those.

3.3. Analysis preparation and reactions

Glass slide for Optical microscopy and Raman spectroscopy

The graphite sample to be analyzed was put on a glass slide and one drop of the reactant liquid was added to the flake with a pipette and then a cover glass was gently placed on top of the flake. The sample setup was then inspected so that the cover glass was lying flat, if the sample is too thick or if the sample is not in the middle of the cover glass the cover glass might tilt and let air in or gas to build up around the sample which might affect the reaction speed. A plastic pincer is used to make any adjustments.

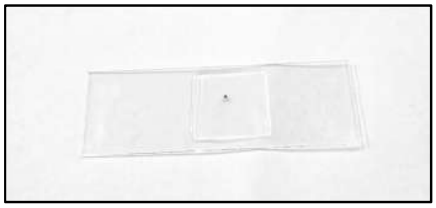

Figure 6. Image of a glass slide, with a 1x1mm HOPG flake with a cover glass on top.

The experimental set-up (*Figure 6*) does not protect the reactant liquid from air, however, the cover glass greatly reduces the contact area between air and the reactant liquid.

Glass vial reactions

The reactions were performed by pouring a reactant mixture prepared according to *3.2 Reagent preparation* into a glass vial and adding a fixed amount of graphite. The glass vial reactions used are listed in *Table 3*.

Table 3. Composition of reagents used in reactions carried out in glass vials.

Vial reaction	Reagent	Amount of reagent (ml)	Graphite (mg)	Reaction time (min)
I	II	1	20	30
II	I	1	20	3hr
III	I	1	20	18hr
IV	VI	1	20	18hr
V	VII-IX	0.89	17.8	1hr and 24hrs

Gas pressure builds up within a matter of hours so the vials must be handled and stored accordingly.

Scale up reaction

For the glass vial reactions listed above used in scale up the vial reaction was performed as described in the previous section and then the material was immersed in a beaker with water 100 times the original reactant volume. Using filter paper (Schleicher & Schuell 595, art. 10311609, 90mm) a büchner funnel and a compressor (ABM Greiffenberger Antriebstechnik F154711, 0.18kW) the material was vacuum filtered and washed, keeping the material wet at all times by adding water by a up to a total volume of 300 times the original. The water is in a large excess to neutralize the acid. After washing with water the pH was about 5. Before finishing filtering, the material was rinsed with ethanol to ease the drying. The material was then left to dry in a semi-closed plastic petri-dish.

XRD sample preparation

The sulfuric acid GIC were prepared according to *vial reaction I*, *Table 3*. About 0.25ml of the reaction mixture together with the flakes were pipetted up and transferred onto a piece of Kapton ® (3M) and then sealed with the tape. The final sample is shown in *Figure 7*.

Figure 7. Prepared sample for XRD analysis. About 3x1cm in size.

The sample provides protection against air moisture and protects the experimental equipment from the reactants.

SEM sample preparation

The sample was prepared by attaching a double adhesive, conductive carbon tape (Agar scientific G3939) to the sample holder and then carefully dipping the holder in a beaker containing the dry graphite material. The sample holder is illustrated in *Figure 8*.

Figure 8. SEM sample holder used during characterization. The diameter of the top flat surface is about 1.5cm.

TEM grid sample preparation

Expanded graphite was added to a vial with water, the vial was shut and sonicated at low power for 2 minutes to exfoliate the material. Using a pincer, a TEM grid was dipped into the solution a few times. The TEM grid was then placed into a custom built sample holder illustrated in *Figure 9*.

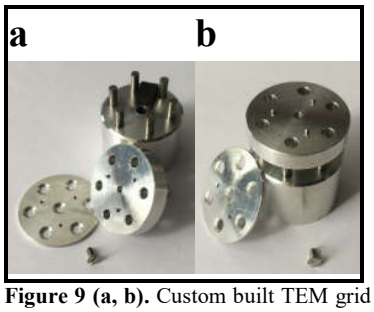

Figure 9 (a, b). Custom built TEM grid sample holder used in SEM. (a) shows the holder taken apart, and (b) shows the holder with the top piece taken off, the grids are placed on the top piece and the top piece is then fastened with the screw illustrated.

3.4. Characterization

Optical microscopy

Optical images were acquired using a Reichet Polyvar-MET equipped with an Inifinity 1 camera and Infinity Analyze 6.5.2 software. Reflective mode was used with a 100W low-voltage halogen lamp light source.

Two types of lenses were used, a Reichert Epiplan 5x for low-magnification imaging and a Reichert Epiplan 25x for higher magnification.

Image analysis

Using images acquired from the optical microscope, several measurements were done.

Calculating the intercalation front speeds

Using a series of photos taken at known times, identifying moving areas in those images, relating them to a non-moving fixed point in the images and a scale-bar makes it possible to calculate the speed of the moving areas. The measurements were done using an in-house script implemented in MatLab.

Calculating the angle based on intensity measurements

Tilting graphite at known angles and taking an image at each angle keeping the camera settings constant will make a reference system for the intensity as a function of angle titled.

Figure 10. Equipment used to measure the tilt angle of the graphite flakes. Consists of a protractor with an attached bracket that has a glass slide taped onto it.

Using the angle device shown in *Figure 10*, taping a glass slide onto it and fixating the samples onto the glass slide makes this possible. A reference system was created and through normalizing the intensities with the maximum intensity at 0°, the system was used for estimating angles in images taken on graphite samples.

Raman spectroscopy

Raman spectra were acquired using a Jobin Yvon Horiba Olympus BX 40 with a Labspec 4.14 software. The instrument was set at 600 grating, 100µm slit and using a 200µm hole and used with a 632.81nm laser. The lens used for orienting at the flake surface was a 100x/0.8 LMPlanFI. At the time of use the spectroscope had a known error, were the true position was shifted, but the relative positions were true. For all measurements made, reference sample was taken using a flaked natural graphite and then the peak positions were shifted relative to that.

SEM and EDX

The data was acquired using a Quanta 3D, Field emission gun (FEG) scanning electron microscope (SEM) (FEI, USA) equipped with an energy dispersive spectroscopy detector: EDAX, (EDAX, USA).

XRD

X-ray diffraction measurements were performed by using a Rigaku Geigerflex powder diffractometer, a focusing beam Bragg-Brentano setup with a graphite-monochromated Cu Kα radiation (λ = 1.5418 Å). The data were collected from 5° to 60° with a 0.02° step and a dwell time of 1s using 40 kV and 30 mA. The samples were sealed in Kapton tape, according to *Method 3.6 XRD sample preparation*.

4. Results

In this section first the analysis of the model system including its optimizations is presented followed by intercalation reactions of graphite for studying the formation dynamics. The chapter is finalized with observations on de-intercalation, expansion of graphite and intercalation reactant compositions.

4.1. Establishing a model system

The initial part focuses on the model system used to study the intercalation of graphite. To understand the behavior of the graphite when subjected to intercalation reactions the following data was collected.

The following three reactions were conducted in the reactional setup described in *chapter 3.3* and with reagents described in *chapter 3.2*.

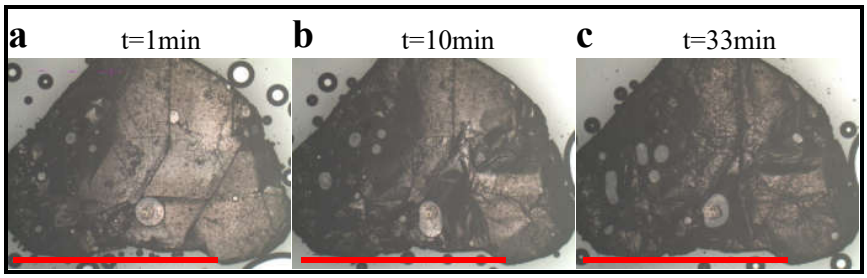

Figure 11 (a, b, c). Graphite reacting in liquid environment, undergoing deformation of the surface. The red bar is 1000µm.

Reacting a graphite flake with *reagent I*, *Table 2*, led to deformation of the surface, however no color phenomena observed after 30 minutes.

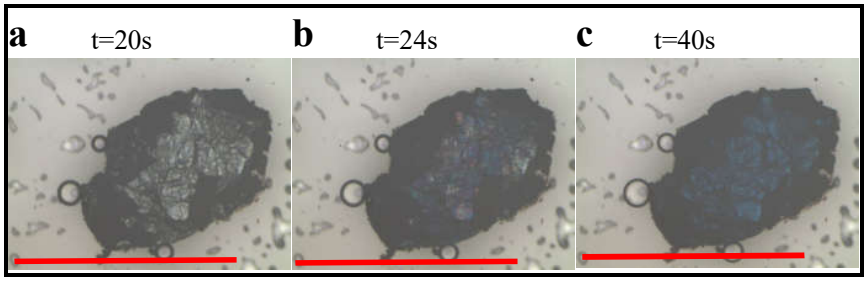

Figure 12 (a, b, c). Graphite reacting in liquid environment, color change in a matter of 24 seconds. The red bar is 1000µm.

Reacting a graphite flake with *reagent II, Table 2*, led to the formation of blue crystals. However, the crystal is blue within 40 seconds of reaction.

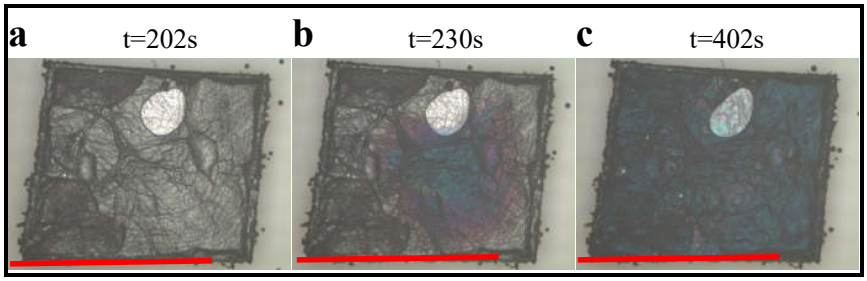

Figure 13 (a, b, c). Graphite reacting in liquid environment, colors appearing at 230 seconds. The red bar is 1000µm.

Using a HOPG sample and reacting with *reagent III*, *Table 2*, made a system with a slower reaction.

Characterization of the intercalation compound

The blue flakes were characterized with Raman, OM and XRD to confirm the staging before the time dependent formation runs were conducted *(chapter 4.2 and 4.3)*. The Raman and OM characterization reactions were conducted in the reactional setup described in *chapter 3.3* and the XRD sample was prepared according to *chapter 3.3* and the reagents used are described in *chapter 3.2*.

Raman and Optical correlation

A glass slide with a HOPG sample was reacted with a reactant mixture according to *reagent IV, Table 2*.

The glass slide was put under the Raman microscope, and for each signal run a confocal measurement was used to determine an approximate intensity focus maximum. Because the intensity decreases for a fixed point over time a constant re-fix of the focal point is needed, and hence the intensity for each measurement cannot be guaranteed to have been at maximum. When a peak shift was detected the glass slide with the sample was moved to an optical microscope and an image acquired.

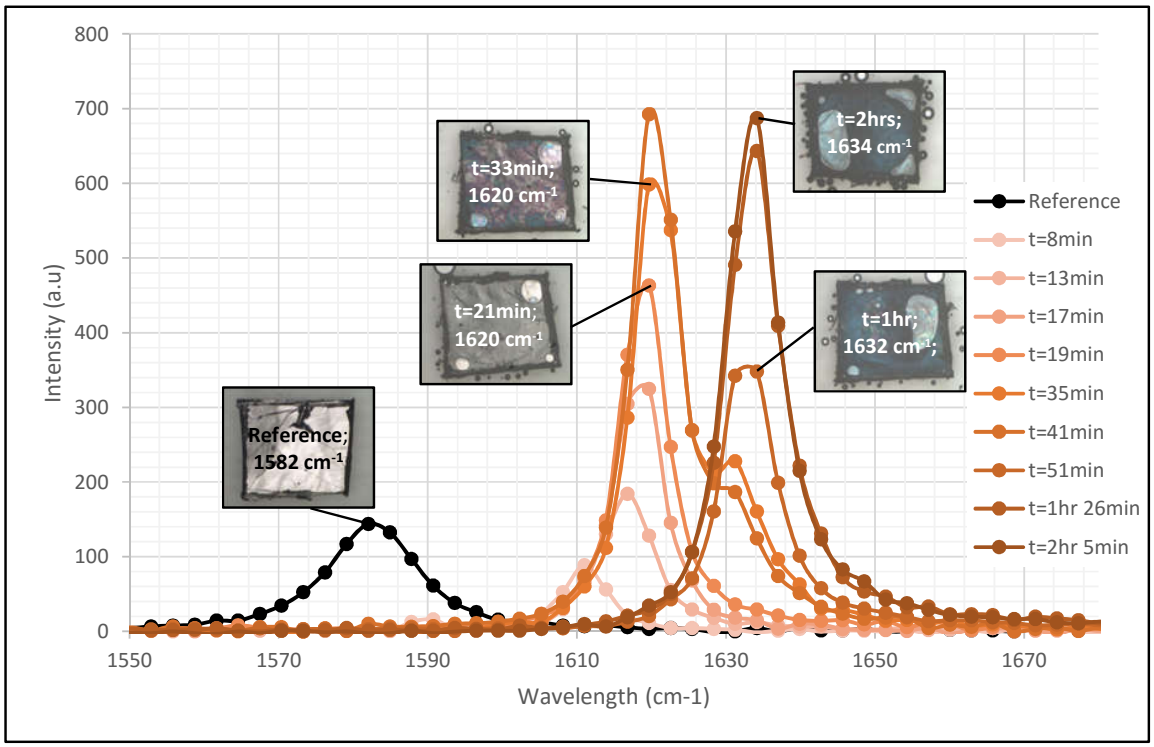

Figure 14. The change in Raman signal as the formation of sulfuric acid GIC proceeds. The flake in the pictures is about 1000µm wide.

An illustration of the appearance of the flake surface in reflective light correlated to the Raman signal acquired around that time is seen in *Figure 14*. The exact time for when the image was taken is shown in the figure and the time for the Raman spectra acquisition can be read in the legend. As the reaction time increases the G peak shifts to a higher wavelength, two distinct peak formations can be seenat 1619 and 1634cm^{-1}. Corresponding to stage-2 and a stage-1, respectively. As intensity shifts to 1634cm^{-1} blue and violet colors on the surface appears and when all intensity is around 1634cm^{-1}, the surface is completely blue.

A confocal analysis was performed on a sulfuric acid GIC, prepared according *vial reaction I, Table 3*.

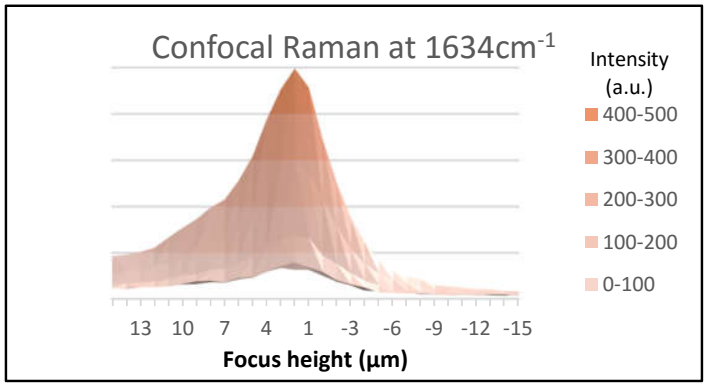

Figure 15. Raman signal measured on a sulfuric acid stage-1 GIC while moving between +15 and -15µm from the position with the highest intensity.

As seen in *Figure 15*, moving into the sample (decreasing the focus height) dampens out the signal after 3µm. Moving out of the sample, a G peak signal can be measured at >10µm. To ensure signal sampling, the focus height needs to be increased as the sample expands.

X-ray diffraction

Sample was prepared according to *chapter 3.3* and analyzed as described in *chapter 3.4* and the results are shown in *Figure 16*.

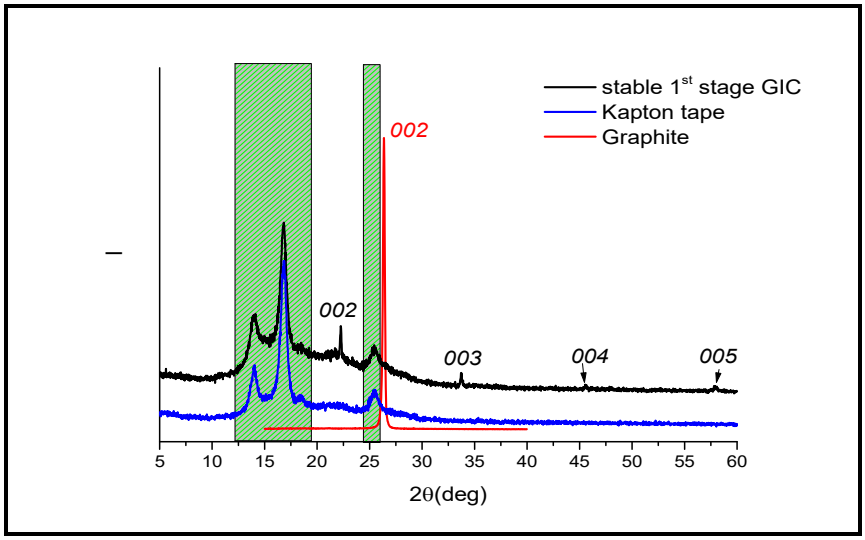

Figure 16. XRD of sulfuric acid GIC (stable 1st stage GIC), graphite reference and a blank sample containing only Kapton ® tape. The green marked regions represent the region from where the signal from the tape is most pronounced.

Looking in *Figure 16* shows the sulfuric acid GIC (stable 1st stage GIC) with diffraction lines detected at ~22.5°, 33.6°, ~45.5° and 55° 2θ angles. The diffraction lines correspond to the 002, 003, 004 and 005 signals respectively. Using Braggs law [24] the c-axis repeat distance I_c was calculated to 0.801nm, which agrees with the stage-1 sulfuric acid GIC according to published data [10], [11].

The results in this chapter forms the basis for the model system used in the two following chapters.

4.2. Monitoring intercalation with Optical microscopy

HOPG flakes were prepared as described in *chapter 3.1*, and cut to about 1.2x1.2mm as seen in *Figure 17*.

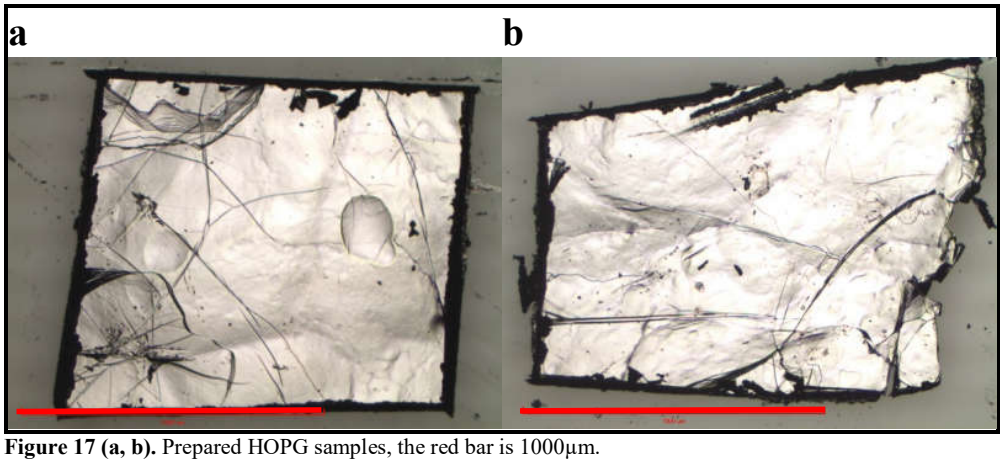

Figure 17 (a, b). Prepared HOPG samples, the red bar is 1000µm.

The samples in *Figure 17* were then mounted according to *chapter 3.3* and reacted with *reagent mixture III, Table 3*, however sample (b) was reacted with a lower concentration of oxidant; using 0.8g ammonium persulfate in the reactant solution preparation. The microscope was then focused on the surface of the flakes and then data collection was started. The data was recorded as a time lapse with a picture taken every 2 seconds and the microscope was used in reflective light mode, according to *chapter 3.4*.

Below are the optical images acquired for when sample in *Figure 17 (a)* is reacted. The images acquired for the reaction of sample in *Figure 17 (b)* is available in *appendix A.2*. A set of fixed frames are presented to show the principle for how the intercalation proceeds in the experiment. The time for the start of the observation is 22 seconds after the addition of the reactant drop onto the flake.

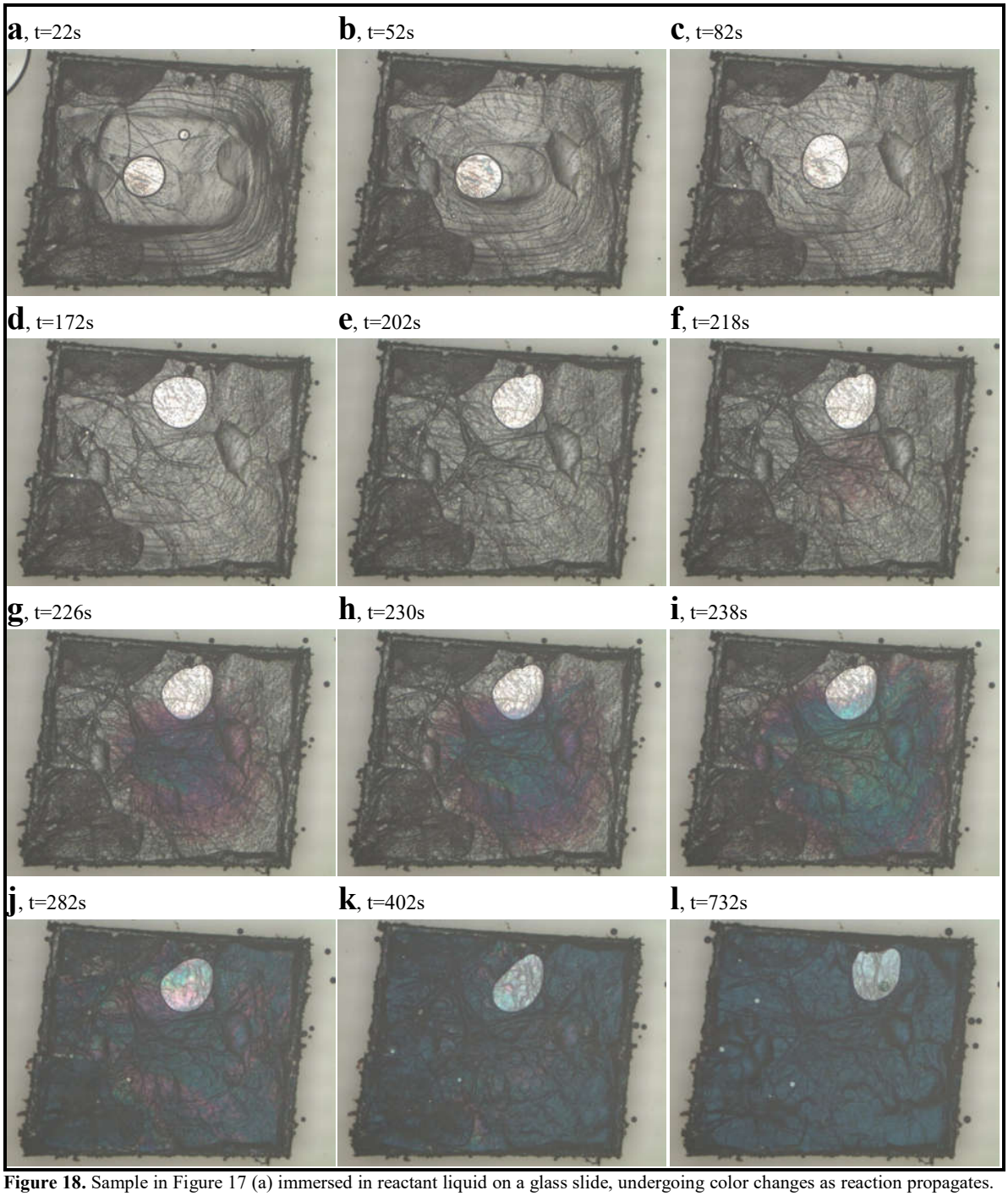

Figure 18. Sample in Figure 17 (a) immersed in reactant liquid on a glass slide, undergoing color changes as reaction propagates. For scale see Figure 17 (a).

Between *Figure 18* (a) and (b) the shifting of a curvature on the surface can be seen, the curvature shift moves from the edges to the center of the flake. In *Figure 19* below is a higher time resolute series illustrating the observed phenomena.

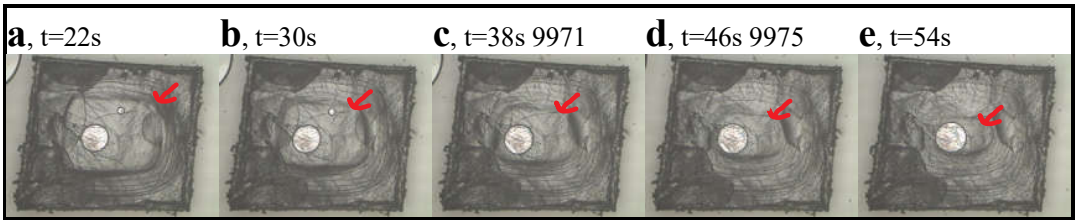

Figure 19 (a-e). Illustrating the surface change over time of a HOPG flake immersed in reactant liquid. The red arrow illustrates the position of the curvature front. For scale see *Figure 17 (a)*.

As time increases the curvature on the surface moves towards the center of the flake *(Figure 19 a-e)* and as the curvature front moves towards the center, a second curvature front can be seen moving in from the edges towards the center. The second curvature front is illustrated in *Figure 20* below.

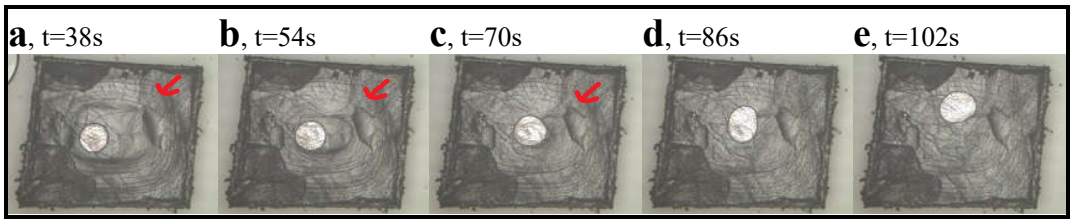

Figure 20 (a-e). Illustrating the surface change over time of a HOPG flake immersed in reactant liquid. The red arrow illustrates the position of the curvature front. For scale see *Figure 17 (a)*.

The curvature fronts are described in more detail in *appendixA.3*. The behavior of a curvature front moving towards the center from the edges was observed for when reacting both samples in *Figure 17* and it happens before the color front appears.
In *Figure 18 (i)* a violet color front appears, which grows greater for each following frame, getting deep blue covering the whole flake in the last frame *Figure 18 (l)*. The color seems to appear from one of the cracks.

Front speeds

Based on the optical observations recorded when samples in *Figure 17* were reacted, the speed of the curvature fronts and color fronts were calculated through image analysis. The speed of the curvature fronts correlates to the intercalation speed. The distance was measured using a fixed point in the middle and then the distance change was measured for a set of images with a known time difference. For specification of which fronts that were measured for each case, see *appendix A.3*. The times are adjusted so that t=0s is the time for when the reactant solution was added to the flake and the data is from when observation was started.
As illustrated in *Figure 19* and *Figure 20*, two curvature fronts were observed moving from the edges towards the center, before the color fronts appeared. These curvature fronts are named G1 and G2 for the first and the second curvature front reaching the center of the flake respectively.

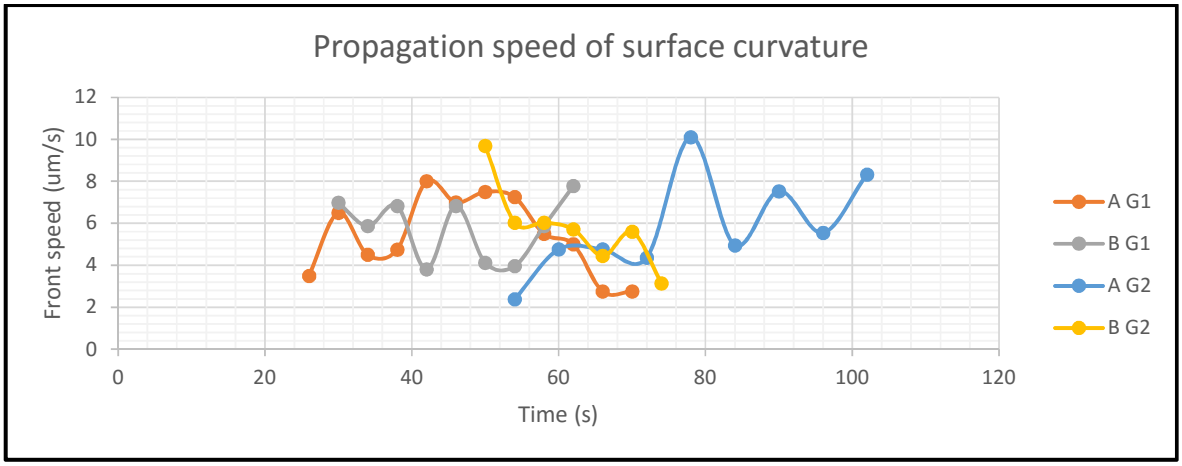

Figure 21. The calculated speeds of the surface curvatures observed when samples in *Figure 17* were monitored during reaction, according to the frames in *Figure 18, denoted A,* and in *appendix A.2, denoted B*. G1 and G2 corresponds to the first and second curvature observed respectively.

From *Figure 21* it can be seen that the speed of propagation is between 3-10µm/s, which is in in the same range as the values measured by *Dimiev et al.* (2-15µm/s) [11]. In *Figure 18*, the speed of the color front was measured starting at *Figure 18 (f)* and then onward. The calculated front speeds are presented in *Figure 22*.

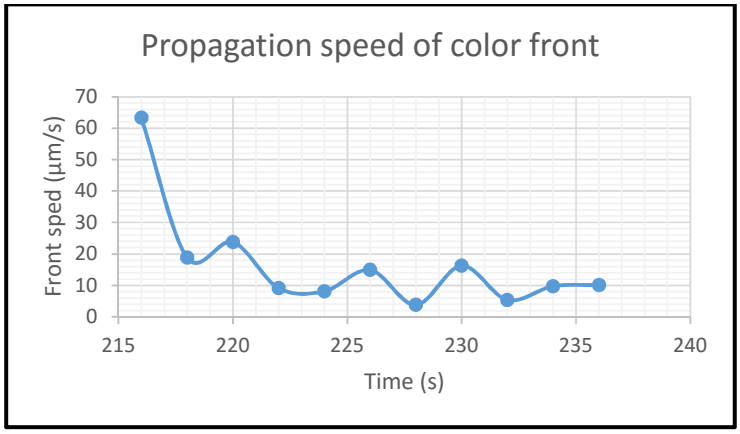

Figure 22. Calculated color front speeds for when sample in figure 1(a) is subjected to intercalation reaction.

The color front appears quickly and had fast initial propagation speeds (>20µm/s) but about 5s after appearing the propagation slowed down to about 10µm/s, the same order of speed as for the grey fronts.

Angle of surface curvature

Tilting the graphite flakes decreases the light being reflected to the direction of the observer. The areas where the surface curvatures are present shows less light intensity, if one assumes that the decrease in light intensity is proportional to the surface curvature, then the angle of the curvature could be approximated. To translate the decreased light intensity to a tilting angle controlled angle intensity measurements as described in *chapter 3.4*, were performed. The resulting data *(Figure 23)* forms an intensity reference system.

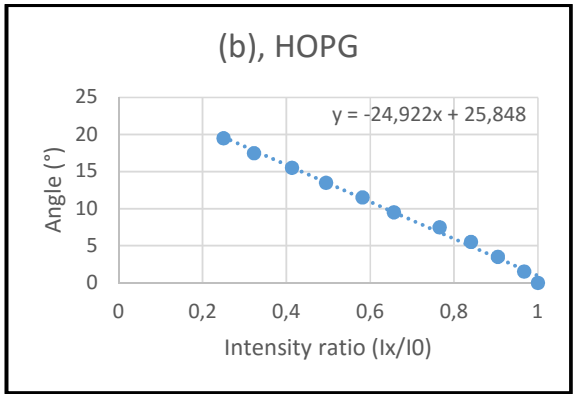

Figure 23. Calculated relation between tilt angle and ratio of the intensity change relative to the intensity at 0°.

There is a linear relation between the tilt and the intensity observed in *Figure 23*. Measuring the intensity at some fixed points were the wave is, and dividing that intensity with the most intense area (corresponding to the 0°) and then using the formula acquired from the reference measurements the angles for the grey waves were approximated, for the measured areas and the calculated angles see *appendixA.4.* Using the angles and approximating the total thickness of the flake being intercalated, a degree of intercalation and hence a staging was approximated.

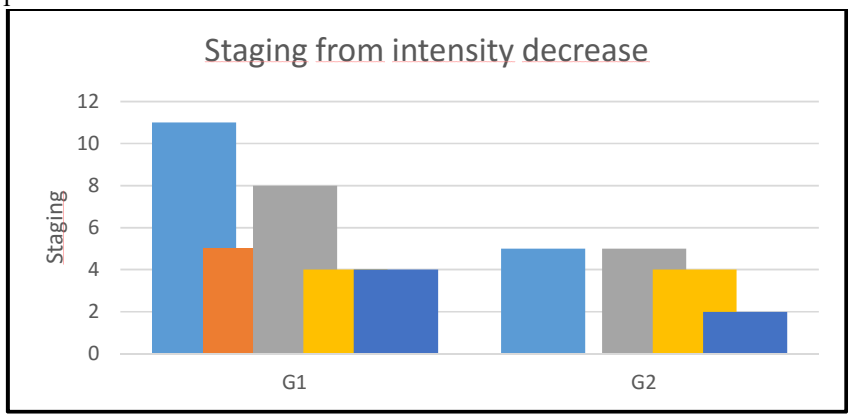

Figure 24. Approximated intercalation staging, based on an approximation of flake thickness, curvature length and angle of curvature.

There is a great variation, but the trend is that the staging is higher for the first grey front. For the first curvature front staging between 4-11 are calculated and for the second curvature front staging between 2-5 are observed. Which is in line with the order of staging propagation from higher to lower *(Figure 1)*.

4.3. Monitoring intercalation with Raman spectroscopy

A HOPG flake was prepared as described in *chapter 3.1*, and cut to about 600x600µm, as seen in *Figure 25*.

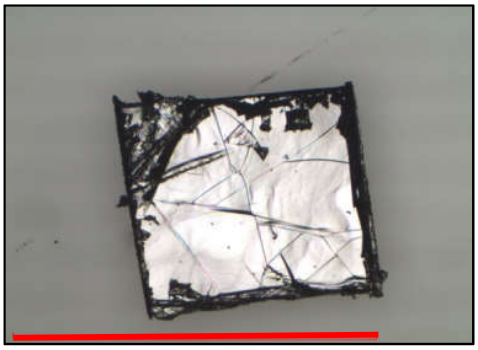

Figure 25. Prepared HOPG sample for Raman intercalation observation. The red bar is 1000µm.

The flake was reacted with reagent III, Table 3 (page 8) and mounted according to *chapter 3.3*. The laser was then focused on the location for maximum signal intensity and then put in signal sampling mode. As stated in the Method chapter, several heights are scanned for each cycle, to make sure that a signal is acquired as the sample is being monitored over time. The following sampling settings were used:

Table 4. Parameters for data acquisition during the Raman spectroscopy measurement.

Sampling time	Sampling cycle time	Sampling depths (µm)	Total sampling duration
1s	10s	0,+2.5,+5,+7.5, +10	1711s

The data acquired from the Raman spectrometer used has a known calibration error and the data has been corrected to that accordingly, as described in *chapter 3.4*. The sampling was started 3 minutes after the drop had been added to the flake.

Signal intensity

The data is acquired as time dependent spectrum series for each sampling height. As seen in *chapter 4.1* the signals of interest are focused around the wavelength of 1600cm^{-1}. The signal intensity between 1539 and 1699cm^{-1}, as a function of time (180-1891s) and observation height (0-10µm) is presented below in *Figure* 26.

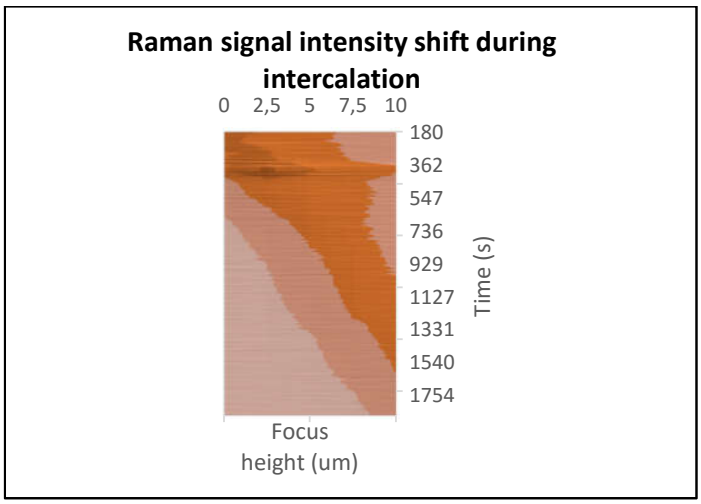

Figure 26. Intensity plotted as a function of reaction time and observation height. Darker orange represents higher intensity.

Looking at *Figure* 26 it can be seen that as time elapses the intensity is shifted in sequental turns from focus height 0 to 2.5, to 5µm and so forth. As shown in *Figure 15* the signal is dampened if the focal point is inside the graphite, hence the results indicates am outward shift of the surface and thus an expansion. Using the data presented in *Figure* 26 a model which relates the height at which maximum intensity is measured as a function of time has been calculated and is displayed below, the calculations are described in *appendix A.5*.

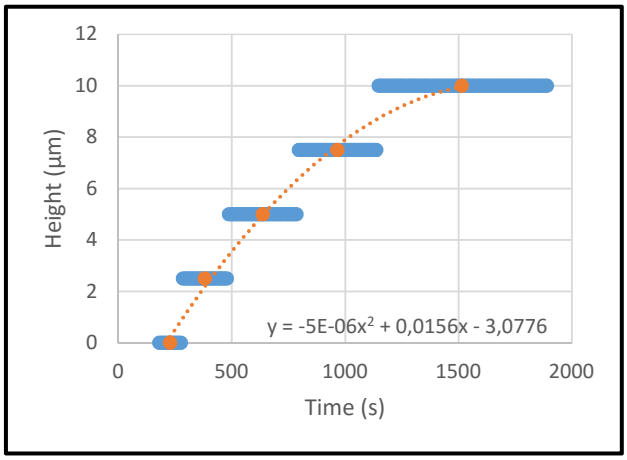

Figure 27. Relation between reaction time and the height, relative to the point for which maximum intensity was measured at the start of the measurements.

The resulting relation describing the height as a function of time was approximated as:

$$h(t) = \ 0{,}0156t \ - 5 \cdot 10^{-6}t^2 - 3{,}0776,$$

where: h = height in µm; t=time in seconds.

Equation 5. A relation between height for maximum intensity measurement as a function of time.

By deriving *Equation 5*, a relation between the speed of intensity height shift as a function of time is acquired.

$$v(t) = 0{,}0156 - 10^{-5}t,$$

where: v = speed in µm/s; t = time in seconds.

Equation 6. The derived expression of *Equation 5*, describing the speed for which the maximum intensity shifts height.

It can be seen that the speed of expansion is highest at the start of the reaction (0.0138µm/s at t=180s) and then is subjected to a constant decrease of speed by 10 pm/s.

G-peak signal shift during intercalation

This section focuses on the Raman spectroscopy signal shift occuring during the stage-2 to stage-1 transition. Using the data presented in the previous section, *Figure* 26, and extracting spectral information in the G-peak region (1580-1640cm^{-1}) at at fixed observation height (+5µm) over time reveals the following information.

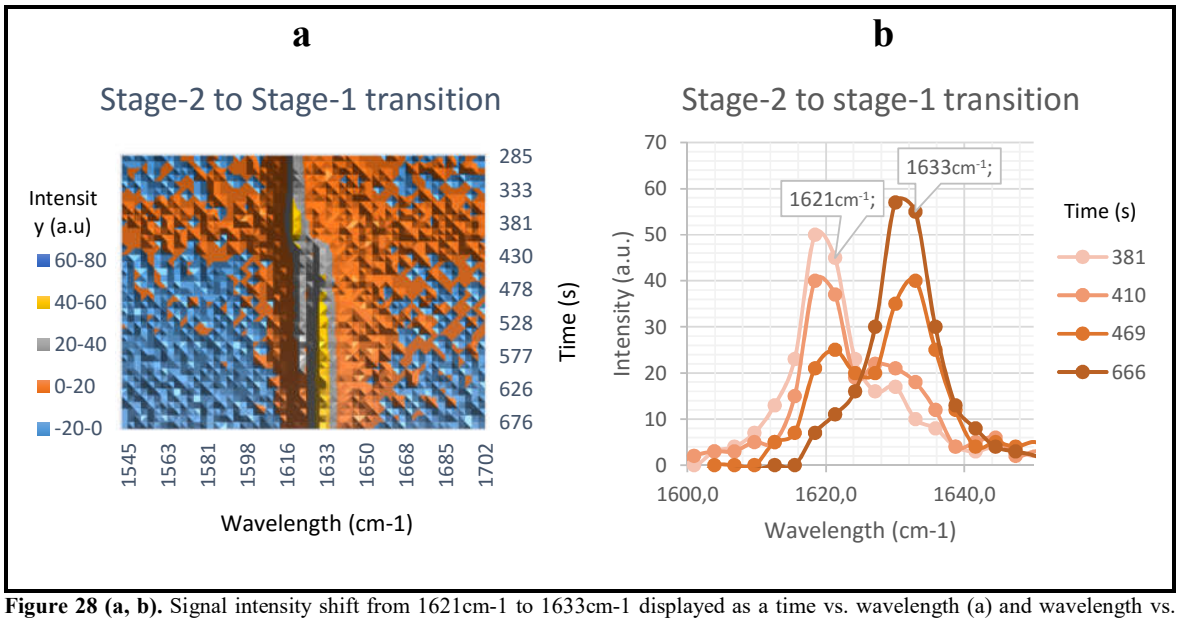

Figure 28 (a, b). Signal intensity shift from 1621cm-1 to 1633cm-1 displayed as a time vs. wavelength (a) and wavelength vs. intensity (b) for the spectrum at 381, 410, 469 and 666 seconds.

In *Figure 28 (a)* it can be seen that the 1621cm^{-1} signal decreases over time and that, starting from approximately 430 seconds the 1633cm^{-1} signal grows in intensity. This is also illustrated in the spectral 2D graph in *Figure 28 (b)*. The 1621cm^{-1} and 1633cm^{-1} signals represent the stage 2 and stage 1 respectively, and so the shift in intesity over time reflects the degree of intercalation as a function of time.

Plotting the intensity for the 1621cm^{-1} and 1633cm^{-1} wavelengths over time for all observation heights shows more clearly the intensity shift, as illustrated in *Figure 29* and *Figure 30*.

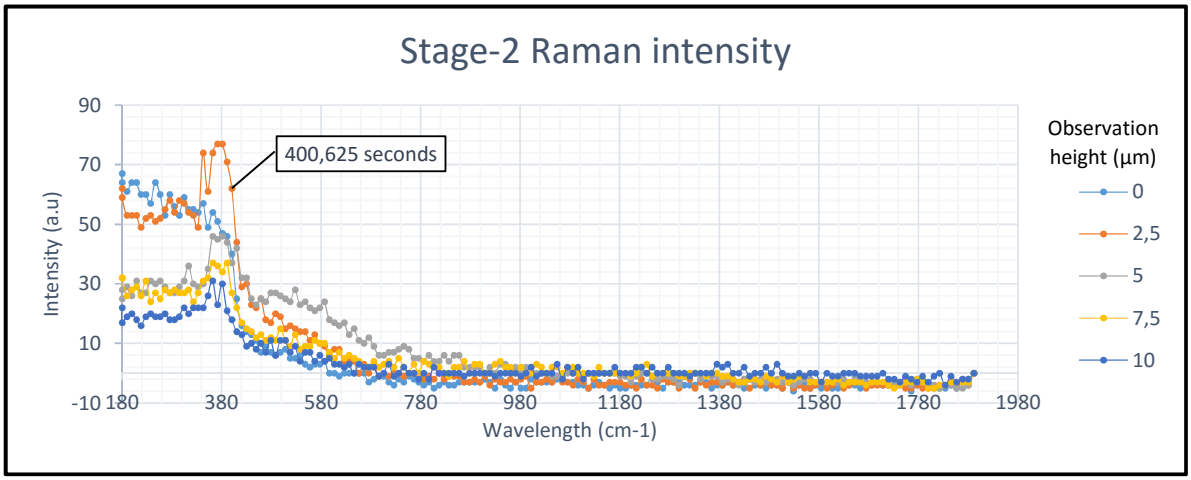

Figure 29. Showing the intensity for the Stage-2 wavelength (1621cm-1) as a function of time. There is a constant decrease in intensity, starting from about 400 seconds for all observation heights.

From about 400 seconds and on, the intensities plotted in *Figure 29* decreases until about 900 seconds, when most of the signal is gone for all observation heights.

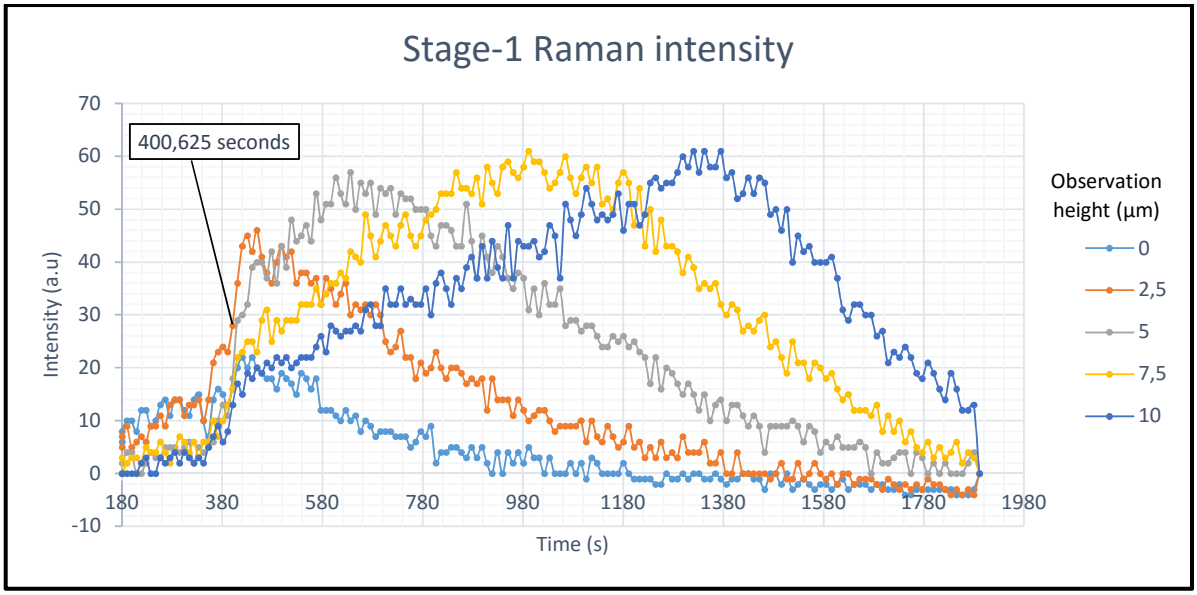

Figure 30. Showing the intensity for the Stage-1 wavelength (1633cm-1) as a function of time. Starting from about 400 seconds for all observation heights there is an increase in intensity until a maximum is reached and then a decrease.

At about 400 seconds there is a distinct overall increase of the intensitties plotted in *Figure 30* for all observation heights, corresponding to the intensity shift from stage-2 to stage-1 as explainged in *Figure 28*. Moreover, for each observation height, there is a intensity maxima and then a decrease. The maximum are found in the order for observation heights from lower to higher, and hence maximum intensity for the observation height 2.5µm is reached before 5µm, and 5µm before 7.5µm and so on. Which is in line with an expanding sample, where the focal point of the Raman signal dampens out as the flake expands and the focal point is inside the sample, as described in *Figure 15*. And consequently the intensity increases for higher observation heights the closer the sample gets to the focal point.

Focusing on the intensity shift from the stage 2 to stage-1 wavelength, a time dependent model for the relative intensity shift was calculated for each observation height. For all models and details regarding the calculations see *appendix A.6*. Here the model for +5µm observation height is presented.

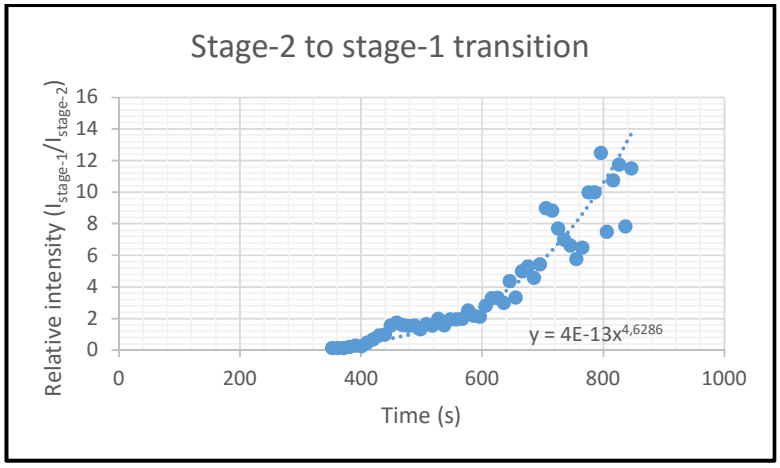

Figure 31. The relative intensity for stage-1/stage-2 sulfuric acid GIC plotted as a function of time. The data is selected during the time frame from about when the shift starts to when the intensity is at or close to zero intensity for the stage-2 compound.

Fitting the data into a model yields the following expression:

$$I_{relative} = 4 \cdot 10^{-13} t^{4{,}628}\ ^{6};\ \text{where } I_{relative} = \frac{I_{Stage\ I}}{I_{Stage\ II}} \text{ and } t = time\ in\ seconds\ (s)$$

Equation 7. Relative intensity for stage-2 and stage-1 sulfuric acid compound as a function of time.

The equation provides a time dependent relation for the lowest stage transition, stage 2 to stage 1.

4.4. De-intercalation and limited staging

Due to the instability of the sulfuric acid GIC (as described in *2.2 De-intercalation*), the material would most likely need to be de-intercalated before use. Also the ability to control the de-intercalation is interesting to control the staging reaction as well as prevent de-intercalation from happening before the reaction is completed. Hence, as follows is the data and observations done during de-intercalation experiments.

Observations with optical microscopy

Graphite flakes were reacted according to *vial reaction II, Table 3*. After the formation was completed, graphite flakes together with reactant liquid were pipetted up and transferred to a glass slide, about 1 drop was added to the glass slide and then a cover glass was put on top.

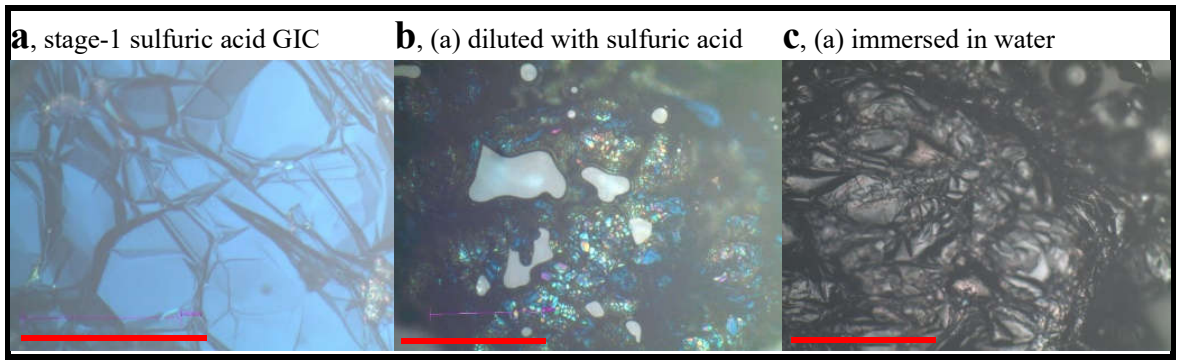

Figure 32 (a, b, c). Images of sulfuric acid GIC stage-1 (a), a sulfuric acid GIC after being diluted (b) and sulfuric acid GIC after being immersed in water (c). The red bar is 100µm.

In *Figure 32 (a)* the surface of the stage-1 GIC after reaction completion is illustrated. Reacted graphite (~10 flakes) were then transferred to a vial with sulfuric acid (2 ml), flakes were then transferred to a glass slide (1 drop and 2 flakes), and are represented in *Figure 32 (b)*. Flakes were then pipetted up and completely immersed in water (100ml), the surface from one of the flakes are presented in *Figure 32 (c)*. The amount of dark blue areas is decreased by sulfuric acid introduction, and completely removed by introducing an excess of water.

A graphite flake prepared as described previously this section (*vial reaction II, Table 3)*, was mounted according to *chapter 3.3*. A drop of water was then added next to the edge of the cover glass. The start time is set for when observation started, the time between the drop was added and for when the observation started was not measured.

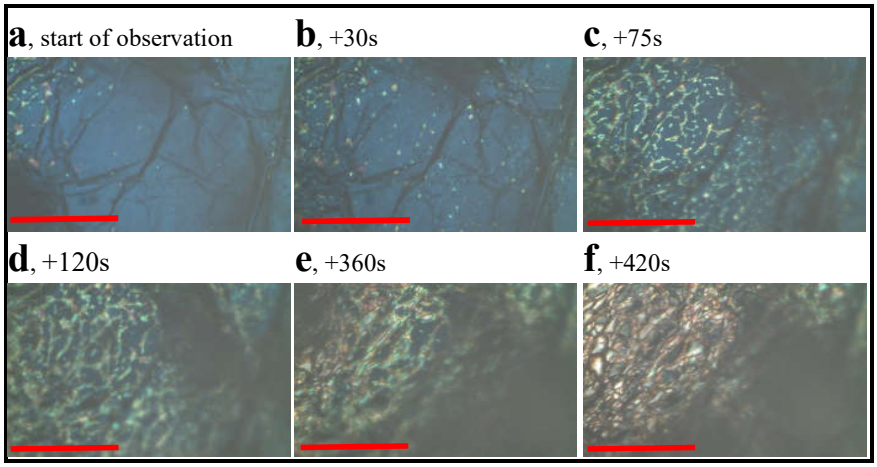

Figure 33. Illustration of water dilution induced de-intercalation of a stage-1 sulfuric acid GIC. The red bar is 100µm.

As time passes the dilution of the reactant mixture increases and the material starts to de-intercalate. As can be seen in *Figure 33* the de-intercalation starts with lighter areas appearing, until the whole surface is covered and then a pink-orange color appears just before the surface becomes grey.

Limiting staging

Three vial reactions were performed according to *vial reaction V, Table 3*. All the reactions use the same concentration of sulfuric acid (diluted with 1/6 molar parts water) and the same amount of graphite, what differs is the concentration of the ammonium persulfate oxidant; 0.87M, 0.44M, and 0.22M respectively. The choice of concentrations is based on the results from *Dimiev et al. (2012, 2015)* where they use a 0.44M solution to achieve a stage-1 compound, and a concentration higher than 0.44M to achieve an over oxidized material and then a lower concentration was chosen as a reference.

After reacting for 24 hours flakes from each vial were pipetted up and mounted according to *chapter 3.3* and the following data was recorded by OM and Raman spectroscopy.

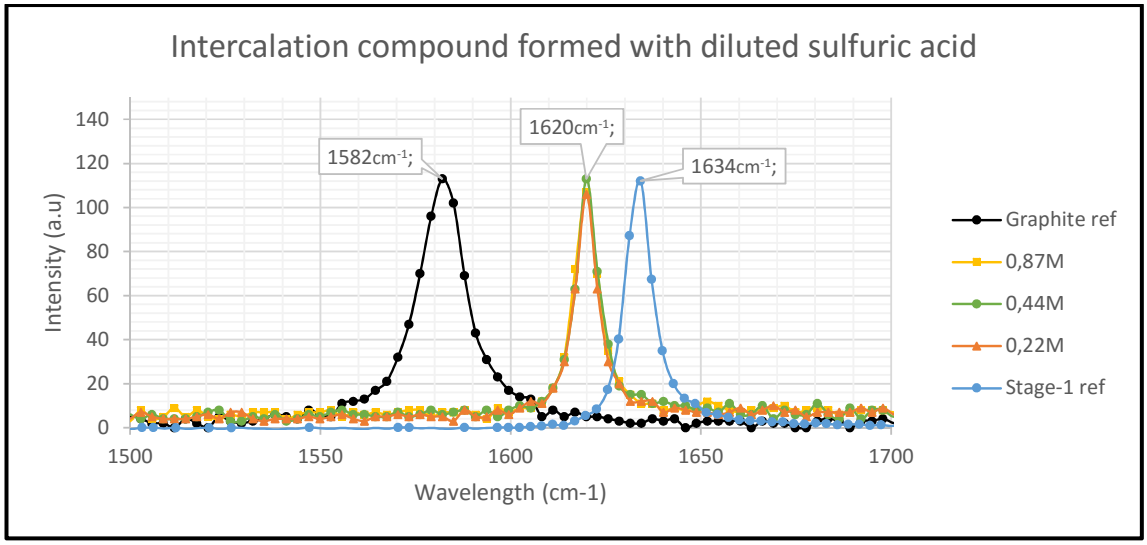

Figure 34. Raman signals acquired for the sulfuric acid GICs formed after reacting in diluted sulfuric acid.

The Raman signals in *Figure 34* are all centered at 1620cm^{-1}, corresponding to a stage-2 compound and indicating that the stage-2 is the dominating stage in the compound.

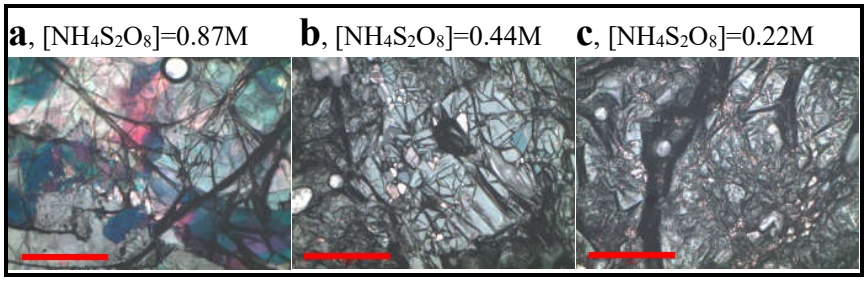

Figure 35 (a-c). Optical images acquired of the surface of flakes from the three different reactions. The red bar is 100µm.

The optical images in *Figure 35* indicates that there is some stage-1 forming for 0.87M but not for 0.44 and 0.22M ($NH_4S_2O_8$).

Raman de-intercalation observations

A HOPG flake was prepared as described in *chapter 3.1,* and cut to about 600x800um, according to *Figure 36*.

Figure 36. Scotch taped and cut HOPG, the red bar is 1000µm.

The flake was reacted with *reagent V*, *Table 3,* and mounted according to *chapter 3.3*. The following points were recorded over time, optical images were only taken in the end due to the de-intercalation happening faster than the time needed to switch between the optical microscope and the Raman spectroscope. The de-intercalation was not induced but happened spontaneously.

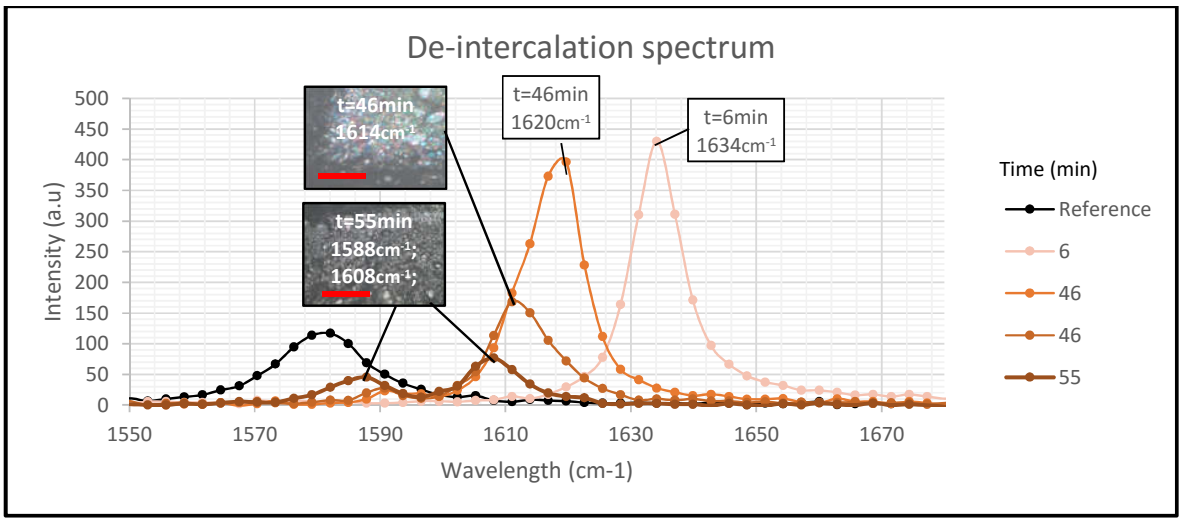

Figure 37. Raman signals and optical images during de-intercalation of a stage-1 sulfuric acid GIC. The red bar in the images is 100µm.

As seen in *Figure 37* the reaction proceeds readily and after 2 minutes a signal at 1634cm^{-1} (stage-1 sulfuric acid GIC) was recorded. The de-intercalation was detected after 46 minutes, when signals at 1619cm^{-1} as well as at 1614cm^{-1} were recorded. At 55 minutes the signal had shifted even lower and the growth of a peak in the graphite region (1582cm-1) started. The de-intercalation and reversion towards graphite is indicated, however, the data only shows de-intercalation for the lower staging and it's not fully de-intercalated in this experiment. De-intercalation initiated by washing with water is handled in *section 4.5* under *Acidic expanded graphite* and *Expansion and non-acidic material*.

4.5. Chemical expansion through oxidizing a stage-1 sulfuric acid GIC

A HOPG flake (also used in *4.4 De-intercalation*) was prepared as described in *chapter 3.1,* and cut to about 600x800µm, according to *Figure 36*. The flake was reacted with *reagent V*, *Table 2* (containing a higher amount of oxidant than used for stage-1 GIC formation) and mounted as described in *chapter 3.3*. The following points were recorded over time by Raman spectroscopy.

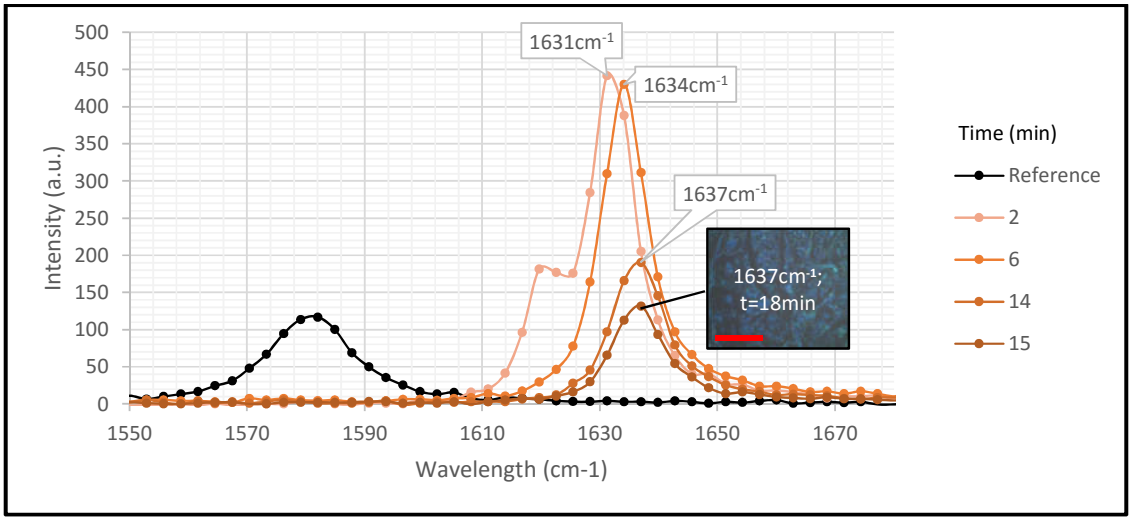

Figure 38. Raman signals measured during oxidation of a stage-1 GIC. The red bar in the image is 100µm.

According to *Figure 38* there is a shift of peak intensity to higher wavelength as well as lowering of intensity. The sample was moved to the Optical microscopy to study the surface change over time.

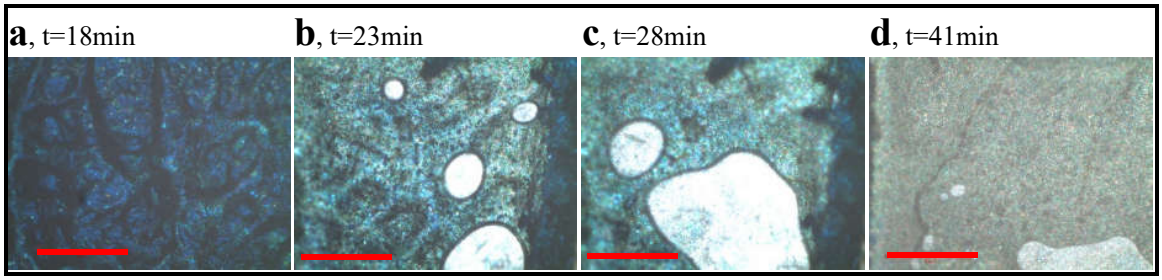

Figure 39 (a, b, c, d). Optical images of surface change of stage-1 GIC as the material is subjected oxidation past stage-1. The red bar is 100µm.

As the reaction proceeds, *Figure 39* illustrates the appearance of light blue regions starting at 18min and then at 41 minutes the whole surface is covered by small light blue regions. The sample then started de-intercalating from the edges, and was put back under the Raman spectroscope (according to *chapter* 4.4 *De-intercalation*).

Acidic expanded graphite

Graphite flakes were reacted according to *vial reaction III and IV, Table 3.*

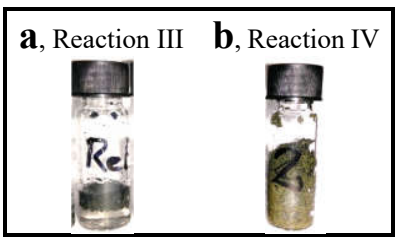

Figure 40 (a, b). Expanded sulfuric acid GIC thorough the oxidation of stage-1 sulfuric acid GIC.

The images in *Figure 40* illustrates that the material from *reaction IV*, *Figure 40 (b),* has by eye acquired more expansion than that of *reaction III, Figure 40 (a)*. The material from *Reaction IV* was then treated according to *3.3 Scale up reaction*, except that the material was not washed or filtered, just immersed in water 100 times the original reactant volume. The pH was measured to be 2. The treated expanded material is referred to as ***sulfuric acid expanded graphite***.

A portion of the sulfuric acid expanded graphite was mounted according to *chapter 3.3.* The following spectra were recorded from three points on a flake, using Raman spectroscopy.

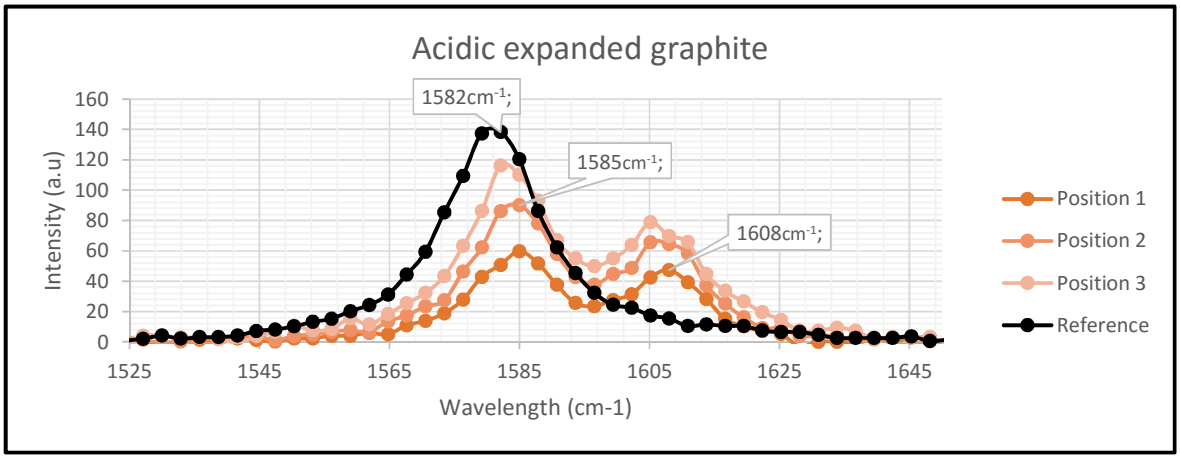

Figure 41. Raman signals acquired from three positions on the surface of the sulfuric acid expanded graphite where the washing water was measured to be at pH 2.

The spectrum in *Figure 41* shows that the sulfuric acid expanded graphite has not the same Raman signal as graphite, but a double peak at 1608cm^{-1} is present as well. Indicating residual intercalant. A portion of the sulfuric acid expanded graphite was prepared for SEM according to *chapter 3.3*. And then the following SEM images were recorded as described in *chapter 3.4 SEM and EDX.*

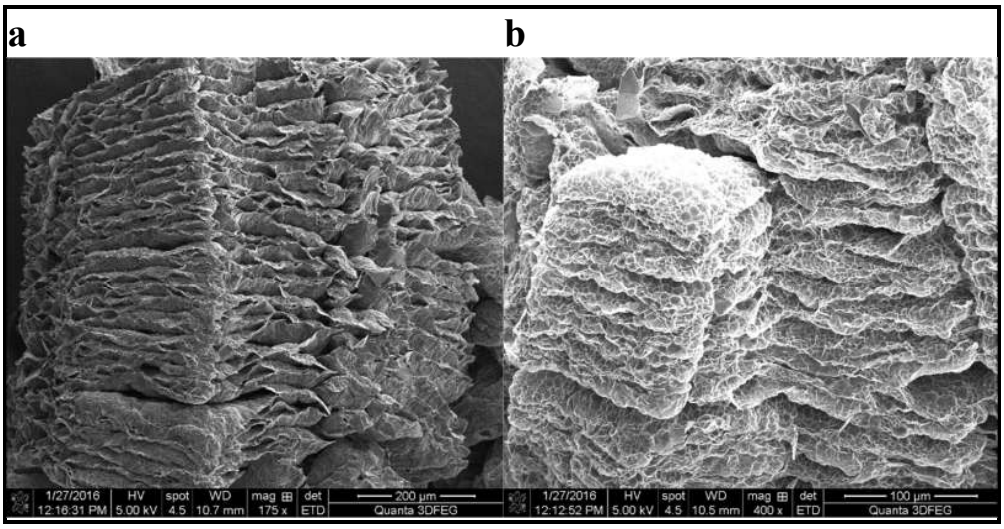

Figure 42. SEM images acquired from the sulfuric acid expanded graphite.

The SEM images in *Figure 42* shows an expanded structure of the graphite were the sheets has started to partly delaminate. For more SEM images see *appendix A.7*.

The sulfuric acid expanded graphite was then put in the microwave and microwaved for about 30 seconds, with light sparkling appearing. The material was then prepared for SEM according to *chapter 3.3*. And the following images were recorded.

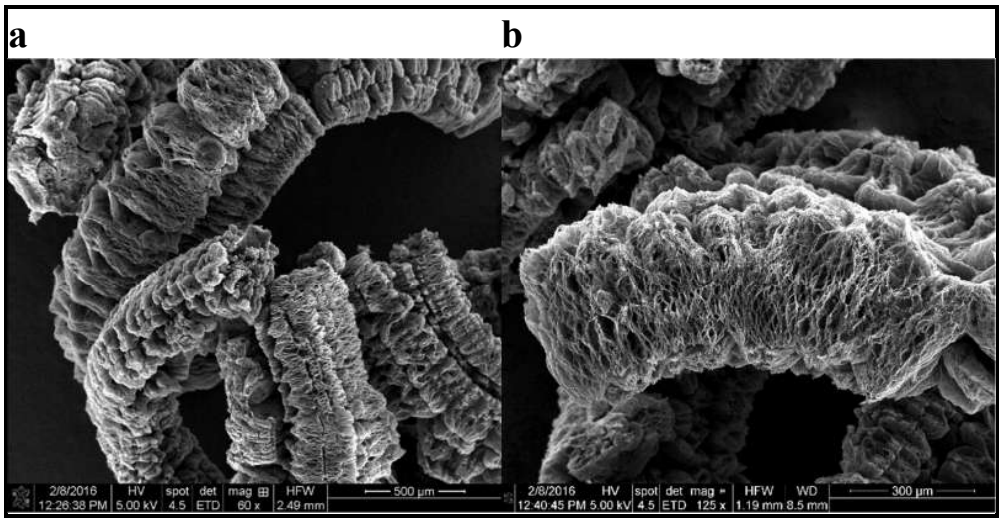

Figure 43. SEM images of microwave treated sulfuric acid expanded graphite.

Comparing the SEM images from *Figure 43* and *Figure 42* shows a more expanded structure in the microwave treated material, however also damage to the surface was observed. For more SEM images see *appendix A.8*.

Expansion and non-acidic material

Graphite flakes were reacted as described in *vial reaction IV, Table 3.* The material was then treated according to *3.3 Scale up reaction*. A portion of the material was then mounted according to *chapter 3.3*. The following spectra was recorded with Raman spectroscopy.

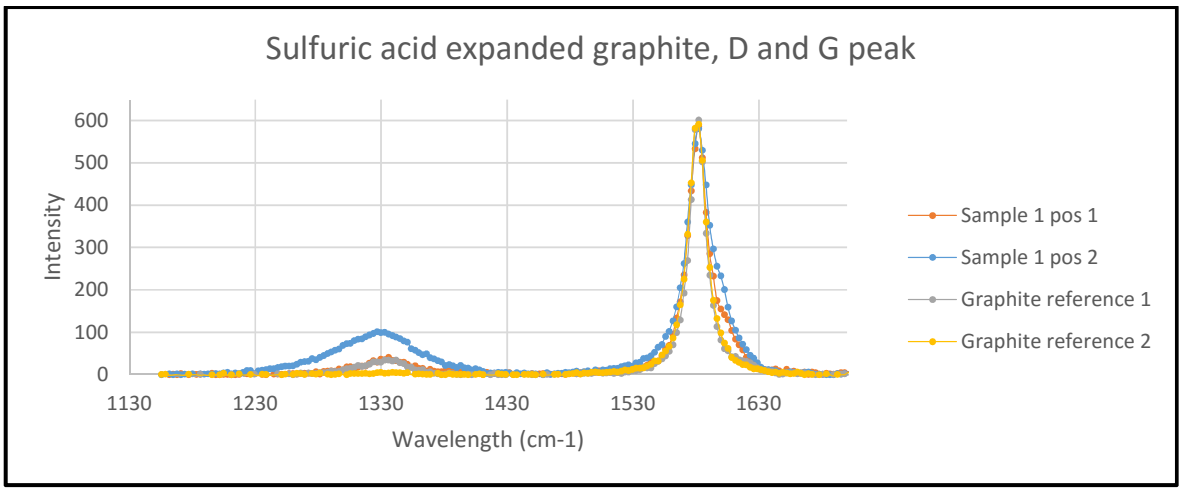

Figure 44. Raman spectrum from sulfuric acid expanded graphite, two sampling positions. The spectrum is focused in the region of the D and G peak. The intensities in all spectra has been normalized to the least intense spectra.

As seen in *Figure 44* there are differences in both the D peak and the G peak between the expanded graphite and the starting material. The G peak is more broadened for the expanded graphite and there's pronounced 'bumps' on the longer wavelength side of the peak. For the full spectra see *appendix A.9.*

Looking at *Figure 42* and *Figure 43* higher contrast areas can be seen. To further analyze them a portion of the sulfuric acid expanded material was mounted according to *chapter 3.3* and SEM and EDX data were recorded according to *chapter 3.4*.

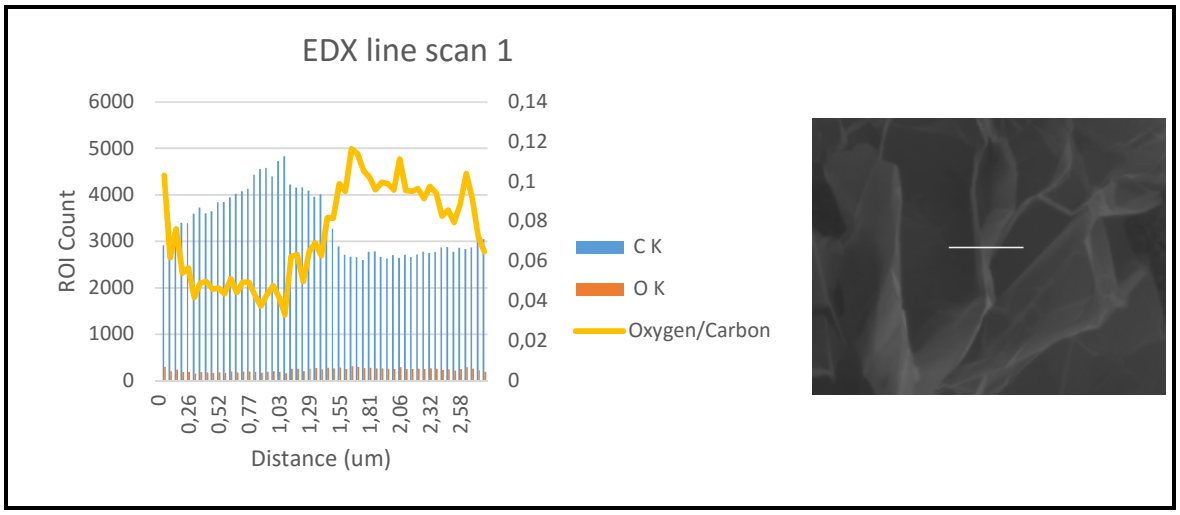

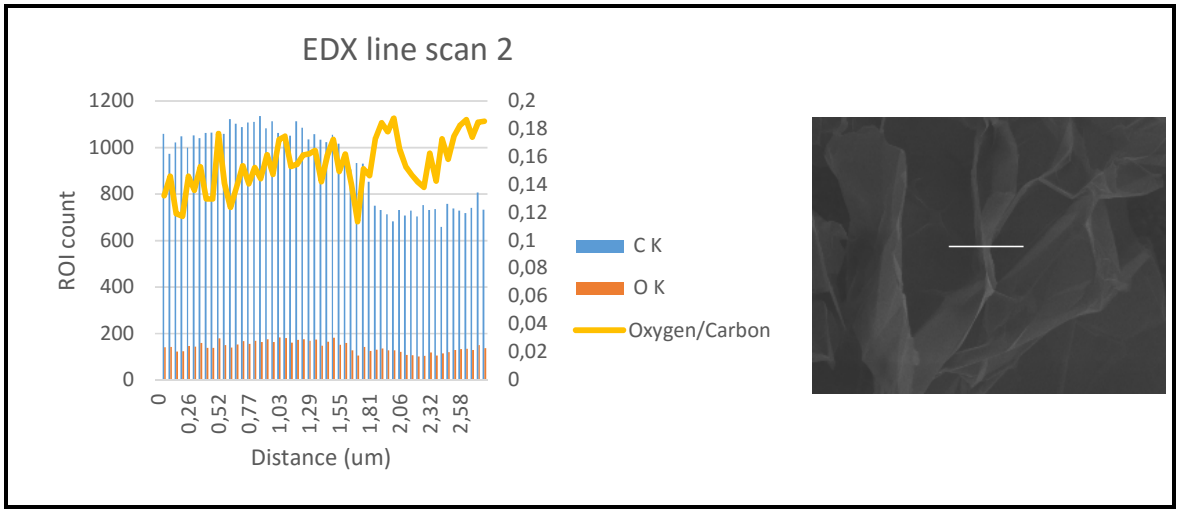

Figure 45. EDX analysis of sulfuric acid expanded graphite. The presence of carbon and oxygen considered and is presented as ROI counts, the ROI count ratio between oxygen and carbon is also displayed.

The fluctuation for oxygen/carbon ratio is most pronounced in line scan 1, however it seems that the fluctuation is due to the change in carbon signal. When the carbon signal drops the oxygen/carbon ratio goes up. The oxygen/carbon ratio varies between 12-18% and 4-12% for line scan 1 and 2 respectively. The sulfur content was also measured; however, the sulfur/carbon ratio was <1% which is below the detectable limit. Details from the analysis can be found in *appendix A.10.*

4.6. Chemical compositions

The direct relation between formation time and concentration of reactants were not fully established, however as follows is the reactant mixtures experimentally used and the response observed.

Glass slide reactions

Table 5. Chemical composition used to create a flake of stage-1 sulfuric acid GIC on a glass slide.

Compound formed	Sulfuric acid (ml)	Oleum (ml)	Ammonium persulfate (g)	Reaction time
Stage-1 GIC	5	5	1-1.25	>20seconds
Stage-1 GIC	10	-	1.25	>60 minutes

The reaction was carried out on a glass slide, according to *chapter 3.3*. As can be seen in *Table 5*, using Oleum (higher sulfuric acid concentration) leads to quicker formation times. The reaction is slower if the amount of oxidant is decreased as well. For reactions not using Oleum the amount of persulfate must be high compared to the ones using Oleum, if decreased the reaction is so slow that it was not visually detected.

Glass vial reactions, stable GIC

Table 6. Chemical compositions used to create the desired sulfuric acid staging compound in a glass vial.

Compound	Sulfuric acid (ml)	Ammonium persulfate (g)	Water (ml)	Graphite (mg)	Ratio oxidant(g)/ graphite(mg)	[persulfate] mol/L	Reaction time
Stage-1 GIC	10	0.5		200	0,0025	0,219	2hrs to 4 days
Stage-1 GIC	5	0.5		200	0,0025	0,438	2hrs to 4 days

Stage-2 GIC	8.3	1.8, 0.9, 0.4	0.56	178	0,0022-0,01	0,22-0,88	2hrs

The vial reactions were carried out according to *chapter 3.3*. Dilution of sulfuric acid led to the formation of a stable stage-2 GIC. Keeping a low ratio between the oxidant and the graphite leads to the formation of a stage-1 compound within 2hrs and keeping the material in the reactant mixture for up to 4 days does not lead to expansion of the material (no further oxidation occurs).

Glass vial reactions, expanded graphite

Table 7. Chemical compositions used to create the desired sulfuric acid expanded graphite compound in a glass vial.

Experiment	H2SO4 95-98% (ml)	NH42S2O8 (g)	Graphite (mg)	Ratio oxidant(g)/ graphite(mg)	[persulfate] mol/L	Reaction time
Double acid #1	2	0,1	20	0,005	0,219	18hrs
Reference	1	0,1	20	0,005	0,438	18hrs
2x excess #3	2	0,2	20	0,01	0,438	18hrs
4x excess #7	4	0,4	20	0,02	0,438	18hrs
8x excess #8	8	0,8	20	0,04	0,438	18hrs
Half acid #4	0,5	0,1	20	0,005	0,877	18hrs
Double oxidant #2	1	0,2	20	0,01	0,877	18hrs

Varying the concentration of ammonium persulfate, leads to different degree of expansion. The critical concentration for a low expansion was found to be 0.22M ammonium persulfate and the highest expansion acquired was for 0.88M ammonium persulfate. The sulfuric acid concentration was kept the same for all experiments.

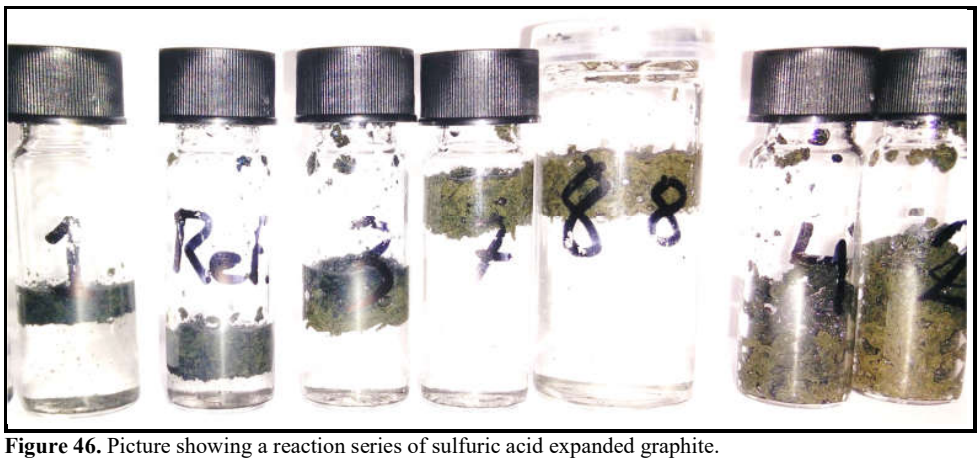

Figure 46. Picture showing a reaction series of sulfuric acid expanded graphite.

The vials shown in *Figure 46* are sorted in order of degree (volume) of expansion, ranging from #1 with the lowest ratio (0.005) and concentration (0.22M) to #2 with the highest ratio (0.01) and concentration (0.88M), as according to *Table 7*. The vials with the highest concentration of persulfate was detected to expand first (#2 and #4) followed by the vials with lower concentration.

5. Discussion

The aim of this work is to investigate the dynamics of sulfuric acid GIC formation to enable industrially scalable production of exfoliated graphite for use in conductive inks. To study the process a model system was chosen, consisting of cut flakes of highly oriented pyrolytic graphite and naturally flaked graphite, reacted with various sulfuric acid and persulfate reactant solutions while monitored and characterized with optical microscopy and Raman spectroscopy. The results discussed below sheds light on intercalation dynamics and methods to control it.

Optical microscopy during intercalation

The optical observations of the intercalation reaction can be summarized as a series of occurrences. First there is a curvature of the surface, propagating from the edges to the center followed by a second curvature moving in the same way. After that cracks are formed and then colors appear. The appearance of color, does not strictly follow the same propagation as the two previous curvature changes. The color appears to start propagating from cracks in the surface. This indicates that the major part of intercalant enters from the edges, along the planes, in the graphite crystal for the higher stagings. While, for the lowest stage transition it seems that cracks in the surface provides the diffusion channel for the intercalant. Weather the cracks were the cause of a structural defect in the crystal or if the cracks were induced due to stress in the crystal as a cause of the expansion has not been determined.

The speed of the curvature and the color fronts gives an order of magnitude for the propagation speed of the intercalation. The timeframe between the different fronts also gives an estimate of the staging shift speed. Due to the fact that recording of the intercalation started about 20 seconds after the reactant mixture, it is possible that there are more curvature fronts than the two observed. The speed (2-8μm/s) of the surface curvature and the movement direction (from the edges to the center) can imply that smaller flakes would be faster intercalated (less distance), hence the size of the flakes would be a critical factor when wanting a homogenous end product with the desired degree of staging.

By using the angle approximation of the curvature, the staging was approximated for the two curvature fronts observed to; G1 4-11 and G2 2-5. The variation of the staging may be either due to the error margin being high, or due to there actually being a mixture of stagings, leading to a change in the curvature as it moves over the surface. However, the results indicate that the waves represent two different groups of stage shifting. The first wave shifts the compound from a staging >10 to a lower ~4 and the second wave shifts the compound from ~4 to 2.

According to *Inagaki et al. (1990)* the intercalation reaction occurs strictly from higher stages to lower stages. Looking at the chemical potential needed for each stage transition in *Figure 2* it can be seen that there is a voltage difference between stage-2 and -1 by 0.5V, between stage-3 and -2 by 0.3V and between stage-4 and -3 by 0.2V. And before stage-4 there was no distinct plateaus. Having that in mind, the first curvature front observed could correspond to the shift from higher stagings to stage-4, after that there is a shift to stage-3 or -2. And finally the color erupts meaning stage-2 to -1 transition. To confirm this, the reaction could be slowed down by decreasing the concentration of persulfate and then perform an in-situ XRD characterization to confirm the stagings as the reaction proceeds, and then match the same experiment with an optical study. Knowing how the reaction proceeds helps in predicting the properties of the resulting material. If a desired staging is wanted in the end material, some of the apparent choices seems to be; staging >10, stage 4, stage 2 and stage 1.

Raman spectroscopy during intercalation

The Raman intercalation results can be summarized in two phenomena, the more intercalated the material is the more shifted the G-peak is and also the more expanded the flake is.

When the signal for a stage-1 compound were acquired the flake was found to still be expanding, this can be related to the fact that Raman spectroscopy only probes about 3µm into the sample *(Figure 15)*. So further into the sample the staging might be lower, which would explain the continuing expansion. The results indicate that surface intercalation is faster than bulk intercalation. The speed of expansion is in the order of 0.0138µm/s and linear (constantly decreasing with 10pm/s), this means that the further the reaction time the slower it goes. Using the average flake thickness of the starting material and calculating the theoretical thickness for a stage-1 intercalated material one can calculate relations such as *Equation 5* and use it to estimate the time for when the expansion is complete (and thus the intercalation).

Two distinct signal maxima were observed which corresponds to the stage-2 and stage-1 peak and for higher stages no such distinct peaks were found. Using the signal intensities for the stage-2 and stage-1 characteristic wavelengths a model that describes the stage shifting was determined as explained in *Figure 31*. The model shows a clear exponential relation between the shift. The model gives an idea of the timeframe for when the stage-1 formation has started and for when it is ended.

De-intercalation and limited staging

The de-intercalation was initiated either by direct dilution with water or it occurred spontaneously. The spontaneity of the de-intercalation was not established; suggestions are, due to moisture in the air or due to consumption of enough oxidant to lower the oxidation potential of the solution. Changing the reduction potential limits the achievable staging. By tuning the reactant composition, the formation of a stable stage-2 compound was performed *(Figure 35)*. The ability to limit the staging is relevant for scalability, when a process which is not sensitive to increase in reaction time is wanted. A multilayered material might be more useful than a single layered material when formulating an ink, because of the multilayered materials greater ability to stack [2].

The de-intercalation was followed by Raman spectroscopy *(Figure 37)* and when comparing the de-intercalation spectrum to the intercalation spectrum *(Figure 14)*, the de-intercalation looks like the reverse mechanism of intercalation. However, the de-intercalation experiments show that higher stagnings of the sulfuric acid GIC is stable in water *(Figure 41)*, and hence even might pose a problem when removal of all intercalants is wanted. When creating an ink, it would probably be desirable to remove the intercalants due to sulfate groups unwanted effect of decreasing the conductivity. There was a correlation between the pH of the washing water and residual intercalant in the material, which also could be measured by Raman spectroscopy *(Figure 41 and Figure 44)*. SEM analysis on acidic, non-fully de-intercalated sulfuric acid expanded graphite showed residue on the surface *(Figure A. 12 (c, d))*, which may be due to the residual intercalants but was not confirmed.

Expansion

Using a higher concentration of oxidant lead to further oxidation of the stage-1 compound. It is confirmed by the further G-speak shift to 1637cm^{-1} *(Figure 38)* in the Raman spectra and also indicated by a surface change observed in optical microscopy *(Figure 39)*. Scaling up this reaction clearly shows an expansion *(Figure 40)* and de-lamination of sheets *(Figure 42)*. The expanded material would need to be further delaminated to be useful in an ink formulation. The de-lamination could be enhanced by using exfoliation techniques as those mentioned in the *Introduction*, but using less power than when exfoliating graphite, because the inter-layer forces are weakened. The exfoliation of expanded graphite would more likely maintain the integrity of the sheets better than when exfoliating graphite.

In the work published by *Dimiev et al. (2015)* [23] an expanded material with a Raman G-peak shift of 1635cm^{-1} is reported, this would mean that the material studied here is more oxidized. Controlling the degree of oxidation is crucial to controlling the characteristics of the produced material. The structural change happening in the material when it goes past stage-1 has not to my knowledge been determined. In the work published by *Shioyamai et al. (1987)* [25] it was observed that the stage-1 sulfuric acid GIC shrank during oxidation, explained by increased attraction between the intercalant and the graphite due to increased charge density of the graphite layers. Shrinking of the material is contradictory to expansion, but the shrinking may be what happens before the sheets starts to delaminate. EDX analysis *(Figure 45)* were used to look into the high contrast folds detected in SEM, it was found that the carbon content decreased right after the fold while the oxygen content stayed constant. The decrease in carbon signal may be due to the fact that less material is present. However, since the oxygen count stays the same, it could mean that the folds are less oxidized. Which would be in the line with the results published by *Dimiev et al. (2015)* [23] which says that the surface of sulfuric acid expanded graphite using persulfate is more oxidized than graphite, but the bulk is still intact. However, to confirm that a more quantitative analysis such as TGA would need to be performed.

Chemical compositions

It was found that a higher concentration of sulfuric acid and persulfate speeds the reaction up. This is in line with Nernst equation *(Equation 2)*. Increasing the concentration of sulfuric acid by using Oleum had a strong effect on the reaction speed *(Table 5)*, from observing blue on the surface within 1 hour to within 1 minute. It was also seen that diluting sulfuric acid limits the staging acquired *(Table 6)*. Finally, by fixing the amount of graphite and the concentration of sulfuric acid and varying the concentration and amount of oxidant leads to different degree of expansion *(Table 7 and Figure 46)*, where the highest expansion is for the reaction with the highest concentration of oxidant and then the limiting factor is the total amount of oxidant used. The more expanded material the more porous, a porous material could be useful in the application as an electrode or a catalyst support. It was also found that tuning the parameters would lead to a stable stage-1 compound with no visible expansion, that material would probably be the least porous and also have more intact layers.

6. Conclusions

Optical microscopy shows that the sulfuric acid graphite intercalation reaction manifests as a curvature front moving (2-8µm/s) over the surface, propagating from the edges to the center followed by a second curvature front moving (3-10µm/s in the same way. After that cracks are formed and then color fronts appears (65µm/s initial speed, stabilizing at 10µm/s). This indicates that the major part of intercalant enters from the edges, along the planes, in the graphite crystal for the higher stagings. While, for the lowest stage transition it seems that cracks in the surface provides the diffusion channel for the intercalants. The staging for the two curvature fronts observed was approximated to stage 11 to 4 for the first curvature front and stage 5 to 2 for the second curvature front.

Raman spectroscopy measurements showed that when the signal for a stage-1 compound was acquired the flake was still expanding. This indicates that surface intercalation is faster than bulk intercalation. The initial expansion speed was found to be 0.0138 µm/s with a constant decrease of the speed by -10pm/s. Two distinct signal peaks were identified in the Raman spectrum at 1633 and 1621cm^{-1}, which corresponds to the stage-2 and stage-1 peaks, no such distinct peaks were found for higher stages.

Using the signal intensities for the stage-2 and stage-1 characteristic wavelengths a model that describes the stage shifting was determined, showing that complete intercalation of the sampling volume was done in 400 seconds after the transition started. The model gives an idea of the timeframe for when the stage-1 formation has started and for when it is ended.

The sulfuric acid GIC de-intercalation Raman spectrum was compared to the spectrum measured during intercalation and found to look like the reverse during the lower stages. However, de-intercalation experiments performed showed that higher stagnings of the sulfuric acid GIC is stable in water, and hence even might pose a problem when removal of all intercalants is wanted.

Using a higher concentration of oxidant (>0.4M $(NH_4)_2S_2O_8$) led to oxidation of the stage-1 sulfuric acid GIC. Performing the expansion reaction in a glass vial with 20mg graphite shows a visually detectable expansion and also de-lamination of sheets confirmed by SEM imaging. Controlling the degree of oxidation is crucial to controlling the characteristics of the produced material.

Keeping the oxidant concentration constant and increasing the concentration of sulfuric acid by adding Oleum had a strong effect on the reaction speed, from observing blue on the surface within 1 hour using 95-98% sulfuric acid to within 1 minute using a 50/50 mixture of Oleum and 95-98% sulfuric acid. By diluting the sulfuric acid in the reactant composition with 1/6 molar parts water, the staging was limited to the formation of a stable stage-2 compound. Varying the concentration (0.2-0.8M) and amount of oxidant affects the degree of expansion, where the most expanded graphite material was found to be produced using a ($(NH_4)_2S_2O_8$ [g])/(graphite [mg]) ratio of 0.005-0.01 and a concentration of oxidant at 0.877M.

The work sheds light on intercalation dynamics and how to control it. This is required when designing a material to be used in a conductive ink formulation in terms of platelet thickness (staging) or a porous material (expansion) and combining this in context of a robust process (time variation tolerant reaction) that is industrially scalable

7. Future work

The work presented here provides a model system that can be used to further study the sulfuric acid GIC formation using optical microscopy and Raman spectroscopy. Based on the results one has a starting point for which reactant compositions to use and the expected results. Apart from that there are also a number of things thats interesting to look more into or develop:

- Developing and investigate the performance of an ink made from the chemically expanded graphite material formed using the intercalation path reported here.
- Further investigate the intercalation in nano-scale with other techniques; LP-TEM, In-situ-XRD
- Study the de-intercalation in more detail to determine how structural defects could be minimized and a good quality material could be produced. For example, studying the material while doing a controlled de-intercalation from oxidized stage-1 GIC to stage-1 and stage-2, studying the surface and material changes while doing so.
- Electrochemical set-up has historically been used to monitor the stage transition, the optical microscopy complements these measurements. But to gain a better understanding of the intercalation phenomena. Coupling an electrochemical set-up with an optical microscope would lead to more detailed knowledge of the propagation of the intercalation and oxidation past stage-1, as well as highly controlled de-intercalation.
- Doing the same experiment as in *chapter 4.3* for a series of reactions with varying concentrations of sulfuric acid and oxidant would enable the construction of a function that describes intercalation staging and expansion as a function of time and reaction composition.

References

[1] A. Capasso, A. E. Del Rio Castillo, H. Sun, A. Ansaldo, V. Pellegrini, and F. Bonaccorso, "Ink-jet printing of graphene for flexible electronics: An environmentally-friendly approach," *Solid State Commun.*, vol. 224, pp. 53–63, Aug. 2015.

[2] A. C. Ferrari et al., "Science and technology roadmap for graphene, related two-dimensional crystals, and hybrid systems," *Nanoscale*, vol. 7, no. 11, pp. 4598–4810, 2014.

[3] M. Cai, D. Thorpe, D. H. Adamson, and H. C. Schniepp, "Methods of graphite exfoliation," *J. Mater. Chem.*, pp. 24992–25002, 2012.

[4] M. S. Dresselhaus and G. Dresselhaus, "Advances in Physics Intercalation compounds of graphite," *Adv. Phys.*, vol. 51, no. 1, pp. 1–186, 1981.

[5] D. D. L. Chung, "A review of exfoliated graphite," *J. Mater. Sci.*, vol. 51, no. 1, pp. 554–568, 2015.

[6] A. M. Dimiev, S. M. Bachilo, R. Saito, and J. M. Tour, "Reversible formation of ammonium persulfate/sulfuric acid graphite intercalation compounds and their peculiar Raman spectra," *ACS Nano*, vol. 6, no. 9, pp. 7842–7849, 2012.

[7] S. Eigler, "Graphite sulphate – a precursor to graphene.," *Chem. Commun. (Camb).*, vol. 51, no. 15, pp. 3162–5, Feb. 2015.

[8] I. Khrapach, F. Withers, T. H. Bointon, D. K. Polyushkin, W. L. Barnes, S. Russo, and M. F. Craciun, "Novel highly conductive and transparent graphene-based conductors.," *Adv. Mater.*, vol. 24, no. 21, pp. 2844–9, Jun. 2012.

[9] W.-C. Oh, N.-K. Bae, Y.-J. Choi, and Y.-S. Ko, "Structural stability and electron energy state of the H2SO4-graphite deintercalation compounds," *Carbon N. Y.*, vol. 33, no. 3, pp. 323–327, 1995.

[10] M. Inagaki, N. Iwashita, and E. Kouno, "Potential change with intercalation of sulfuric acid into graphite by chemical oxidation," *Carbon N. Y.*, vol. 28, no. 1, pp. 49–55, 1990.

[11] A. M. Dimiev, G. Ceriotti, N. Behabtu, D. Zakhidov, M. Pasquali, R. Saito, and J. M. Tour, "Direct real-time monitoring of stage transitions in graphite intercalation compounds," *ACS Nano*, vol. 7, no. 3, pp. 2773–2780, 2013.

[12] F. Minisci, A. Citterio, and C. Giordano, "Electron-transfer processes: peroxydisulfate, a useful and versatile reagent in organic chemistry," *Acc. Chem. Res.*, vol. 16, no. 1, pp. 27–32, Jan. 1983.

[13] D. A. House, "Kinetics and Mechanism of Oxidations by Peroxydisulfate.," *Chem. Rev.*, vol. 62, no. 3, pp. 185–203, Jun. 1962.

[14] R. W. Scott, Paula, Rosanne Menzel, Robert Mullholand, "Persulfates Technical information," vol. 22, no. 3, pp. 141–142, 2001.

[15] C. Rigaux, "The weak interlayer interactions allow the intercalation of a wide diversity of atomic and molecular spe des between the carbon layers. Graphite," *Intercalation Layer. Mater.*, vol. 148, pp. 235–255, 1986.

[16] M. Saint Jean, M. Menant, N. H. Hau, C. Rigaux, and A. Metrot, "In situ optical study of H2SO4-graphite intercalation compounds," *Synth. Met.*, vol. 8, no. 1–2, pp. 189–193, Dec. 1983.

[17] M. M. Lucchese, F. Stavale, E. H. M. Ferreira, C. Vilani, M. V. O. Moutinho, R. B. Capaz, C. A. Achete, and A. Jorio, "Quantifying ion-induced defects and Raman relaxation length in graphene,"

Carbon N. Y., vol. 48, no. 5, pp. 1592–1597, 2010.

[18] L. G. Cançado, A. Jorio, E. H. M. Ferreira, F. Stavale, C. A. Achete, R. B. Capaz, M. V. O. Moutinho, A. Lombardo, T. S. Kulmala, and A. C. Ferrari, "Quantifying defects in graphene via Raman spectroscopy at different excitation energies.," *Nano Lett.*, vol. 11, no. 8, pp. 3190–6, Aug. 2011.

[19] A. M. Dimiev, G. Ceriotti, N. Behabtu, D. Zakhidov, M. Pasquali, R. Saito, and J. M. Tour, "S Direct real-time monitoring of stage transitions in graphite intercalation compounds," *ACS Nano*, vol. 7, no. 3, pp. 2773–2780, 2013.

[20] A. C. Ferrari, "Raman spectroscopy of graphene and graphite: Disorder, electron-phonon coupling, doping and nonadiabatic effects," *Solid State Commun.*, vol. 143, no. 1–2, pp. 47–57, 2007.

[21] P. C. Eklund, C. H. Olk, F. J. Holler, J. G. Spolar, and E. T. Arakawa, "Raman scattering study of the staging kinetics in the c-face skin of pyrolytic graphite-H2SO4," *J. Mater. Res.*, vol. 1, no. 02, pp. 361–367, 2011.

[22] P. C. Eklund, C. H. Olk, F. J. Holler, J. G. Spolar, and E. T. Arakawa, "Raman scattering study of the staging kinetics in the c-face skin of pyrolytic graphite-H2SO4," *J. Mater. Res.*, vol. 1, no. 02, pp. 361–367, Jan. 2011.

[23] A. M. Dimiev, G. Ceriotti, A. Metzger, N. D. Kim, and J. M. Tour, "Chemical Mass Production of Graphene Nanoplatelets in □100% Yield.," *ACS Nano*, Nov. 2015.

[24] E. Lifshin, Ed., *X-ray Characterization of Materials*. Weinheim, Germany: Wiley-VCH Verlag GmbH, 1999.

[25] H. Shioyama and R. Fujii, "Electrochemical reactions of stage 1 sulfuric acid—Graphite intercalation compound," *Carbon N. Y.*, vol. 25, no. 6, pp. 771–774, 1987.

A. Appendix 1

A.1. Sample preparation

Cut natural graphite

Cutting graphite samples from a crystal of natural graphite with a scalpel was problematic since there were difficulties to get a homogenous thickness which induced problems when observing the sample with optical microscope, due to a lot of the light being reflected away due the surface not being flat.

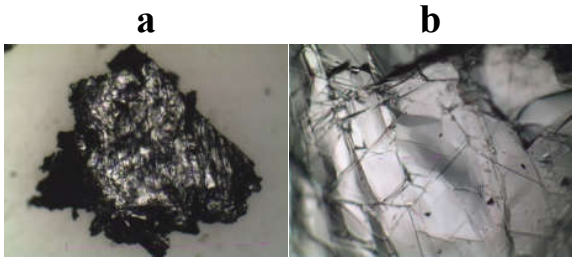

Figure A. 1 (a, b). Natural graphite.

Flaked natural graphite

Flaked graphite showed more homogenous of thickness and surface morphology on a macroscopic scale, however on a microscopic scale a lot of defects were found.

Figure A. 2 (a, b). Flaked natural graphite.

Scotch taped, flaked natural graphite

Scotch taping flaked natural graphite yielded a more homogenous material on the microscopic scale, in comparison to the non-scotch taped flake.

Figure A. 3 (a, b). Flaked natural graphite (a) before and (b) after scotch tape treatment.

Scotch taped, cut HOPG

Scotch taping HOPG and cutting the flake to fit the sample size yielded an optically homogenous material.

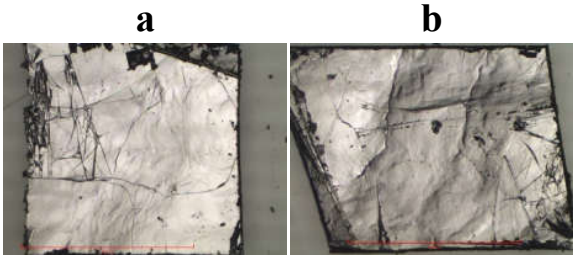

Figure A. 4 (a, b). HOPG, scotch taped and cut.

A.2. OM during HOPG flake intercalation

The sample *(Figure 17 (b), page 15)* was prepared and reacted as described under *Results 4.2 Monitoring intercalation with Optical microscopy (page 15)*.

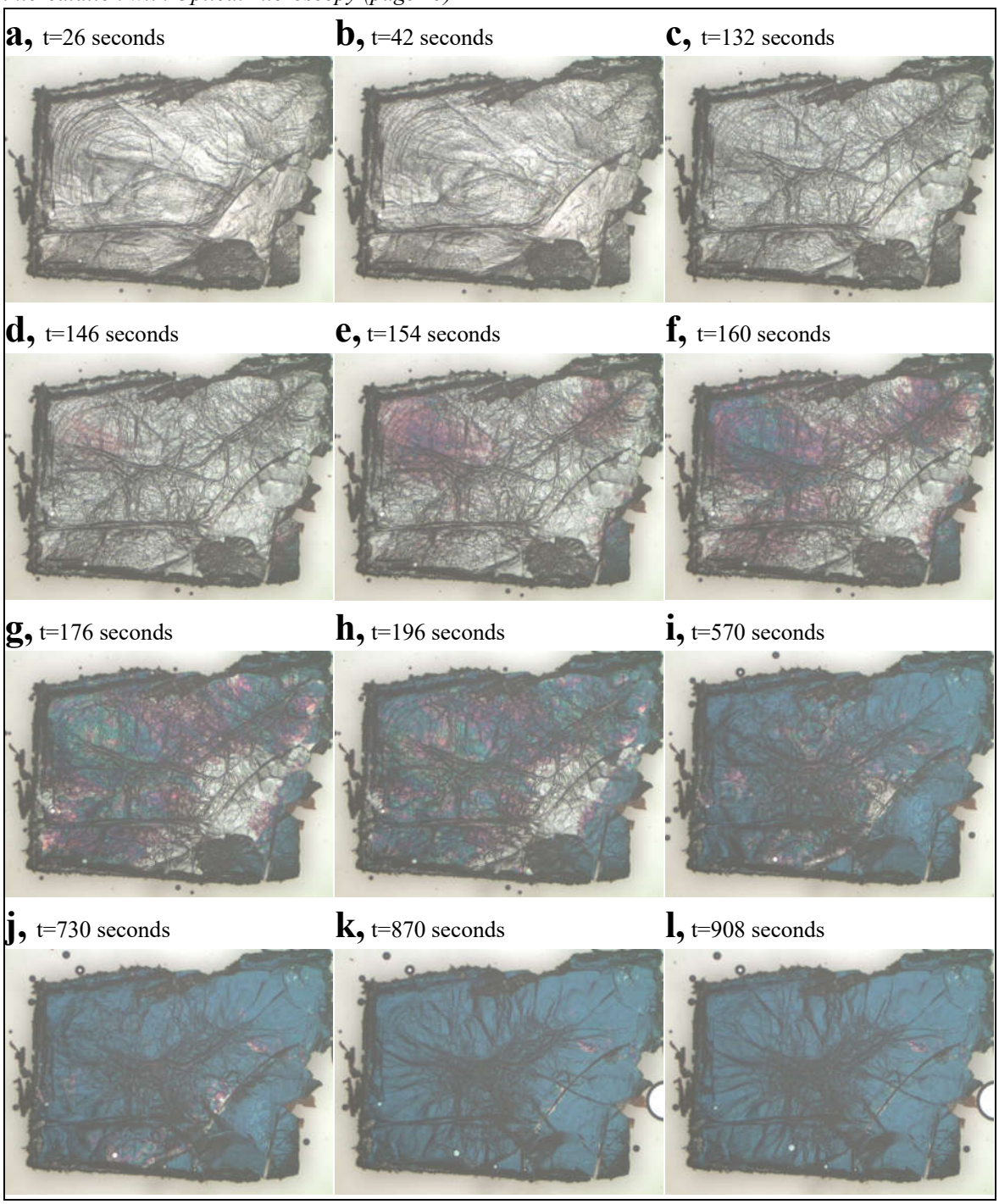

Figure A. 5 (a-l). HOPG flake intercalating in a liquid environment on a glass slide with a cover glass on top.

A.3. Intercalation front speed calculations

Illustrating were the surface curvatures has been identified. For a better understanding, study the frames attached in Figure 18 (page 16) and Figure A. 5 (page 41), or consider the video in the digital supplemental. For each frame, the position of the curvature front to a fixed point in the center was measured. Between each frame there is a time delay of 2 seconds, and by dividing distance with time the surface curvature speed was calculated.

Flake in *Figure 17 (b)* intercalating

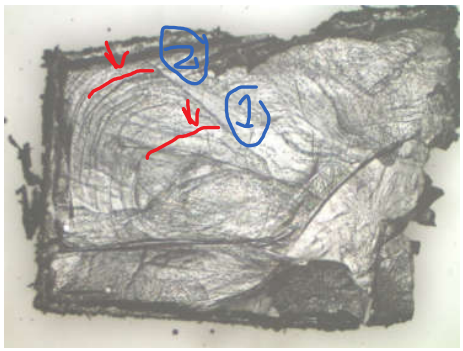

Figure A. 6. Showing the surface curvature G1 (1) and G2 (2), as time progresses the curvature moves towards the center. The red arrows points towards the moving direction of the surface curvature.

Parameters for data capture (flake in *Figure 17 (b)* intercalating): time lapse was started 26 seconds after the reactant mixture and cover glass was added onto the flake. The time lapse was recorded for a total of 18 minutes and 10 seconds. The data was recorded using a magnification of 5x0.8.

Flake in *Figure 17 (a)* intercalating

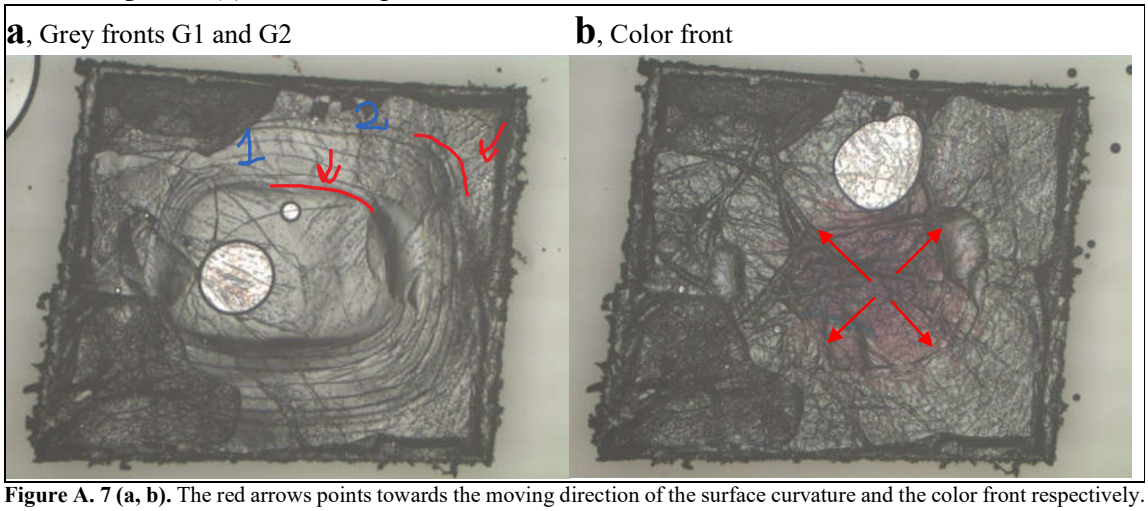

Figure A. 7 (a, b). The red arrows points towards the moving direction of the surface curvature and the color front respectively. (a) Showing the surface curvature G1 (1) and G2 (2), as time progresses the curvature moves towards the center. (b) Showing the color front in the center.

Parameters for data capture (flake in *Figure 17 (a)* intercalating): time lapse was started 22 seconds after the reactant mixture and cover glass was added onto the flake. The time lapse was recorded for a total of 16 minutes and 13 seconds. The data was recorded using a magnification of 5x0.8.

A.4. Surface curvature calculations

Flake intensity measurements and corresponding angle

The intensity was measured in the boxes marked in the images below, the whole box was not measured, the box is more indicative for where the curvature or the reference area is. The reference area is selected so that it's approximately the brightest area in the image. The angle of the curvature was calculated using the linear relation acquired from *Figure 23 (page 19),* diving all the measured intensities with the reference intensity to get a ratio, and then enter the ratio in the relation to get the angle.

Flake in *Figure 17 (a)* intercalating.

a, G1

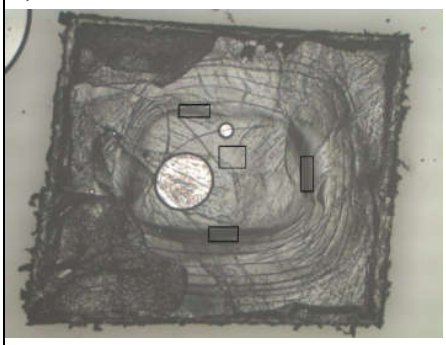

Measured intensity (a.u.)	Calculated angle (°)
172,1	-
116,6	8,9
95,3	12,0
98,9	11,5

b, G2

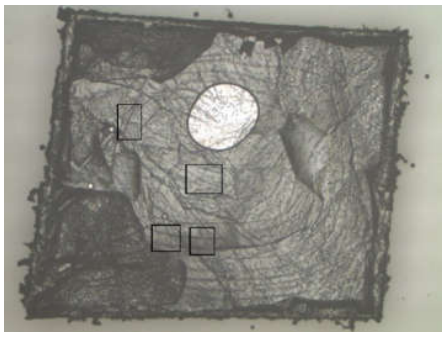

Measured intensity (a.u.)	Calculated angle (°)
162,7	-
135,1	5,2
125,9	6,6
105,0	9,8

Figure A. 8. The areas for which the intensity was measured and corresponding angle was approximated. (a) measured the first curvature front and (b) measures the second curvature front.

Flake in *Figure 17 (b)* intercalating.

a, G1

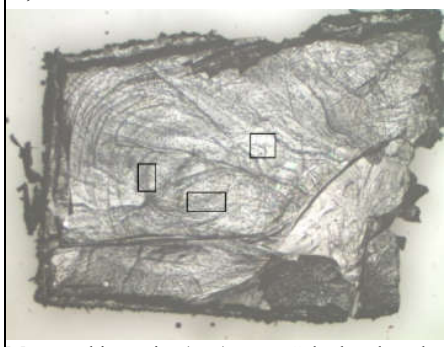

Measured intensity (a.u.)	Calculated angle (°)
235,5	-
187,6	5,9
158,9	9,0

b, G2

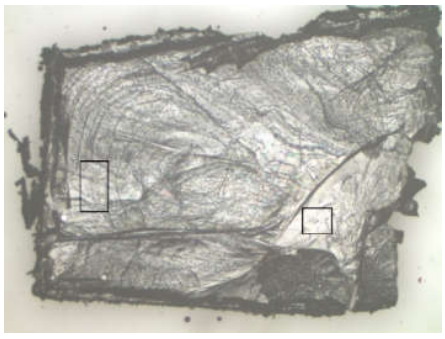

Measured intensity (a.u)	Calculated angle (°)
243,9	-
196,4	5,8

Figure A. 9. The areas for which the intensity was measured and corresponding angle was approximated. (a) measured the first curvature front and (b) measures the second curvature front.

Flake staging approximation from calculated angles

The thickness of the flakes in *Figure 17* was approximated using OM and tilting the HOPG flake.

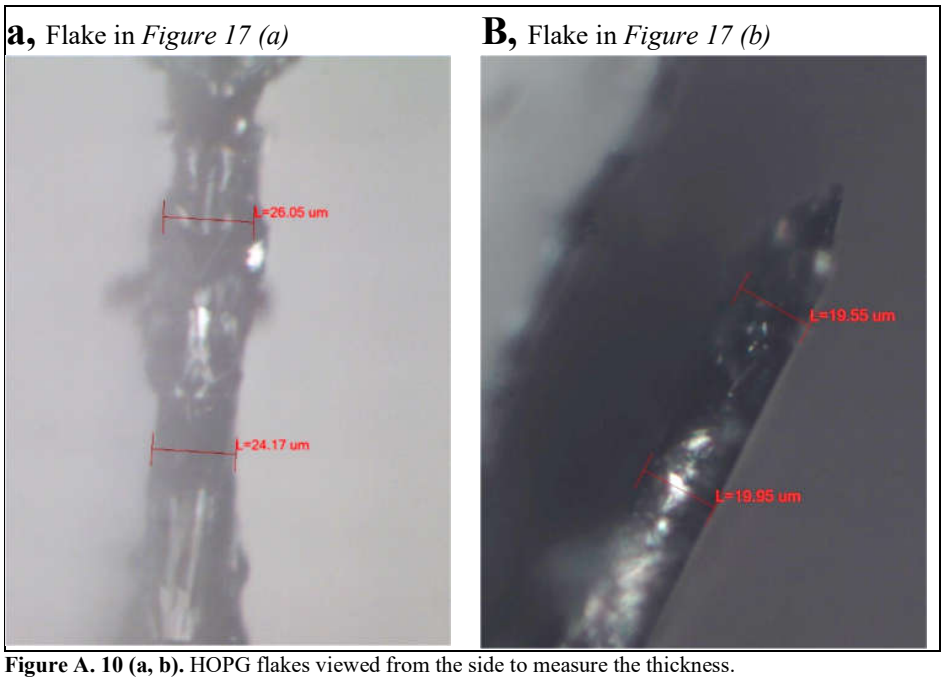

Figure A. 10 (a, b). HOPG flakes viewed from the side to measure the thickness.

According to *Figure A. 10* the flake in *Figure 17 (a)* is ~25µm and the flake in *Figure 17 (b)* is ~20µm.

Approximating the length of the surface curvature, together with the calculated angles presented in *Figure A. 8* and *Figure A. 9* gives an approximation of the thickness increase that the curvature gives rise to. Assuming that this thickness is due to intercalation, that the whole flake intercalates homogenously and knowing the original thickness of HOPG, gives an order of the staging. The following table is the results of those calculations and the basis for Figure 24 (page 19). To calculate the staging the thickness of the intercalant (0.466nm) and the distance between the graphite layers (0.335nm) was retrieved from the references [11].

Table A. 1. The data and calculated values for approximating the staging. The sample is *Figure 15 (a)*, and the angles and lengths has been measured in *Figure A. 8*.

Curvature front	Angle (°)	Length (µm)	Height (µm)	Intercalant layers (#)	Graphite layers (#)	Staging
G1	9,0	26,4	4,1	8839,0	74626,9	8,4
G1	12,0	44,1	9,2	19727,8	74626,9	3,8
G1	11,5	47,3	9,4	20272,3	74626,9	3,7
G2	5,2	72,1	6,5	13921,7	74626,9	5,4
G2	6,6	73,7	8,4	18106,3	74626,9	4,1
G2	9,8	92,9	15,8	33827,5	74626,9	2,2

Table A. 2. The data and calculated values for approximating the staging. The sample is *Figure 15 (b)*, and the angles and lengths has been measured in *Figure A. 9*.

Curvature front	Angle (°)	Length (µm)	Height (µm)	Intercalant layers (#)	Graphite layers (#)	Staging
G1	6,0	24,8	2,6	5561,7	59701,5	10,7
G1	9,0	36,1	5,7	12150,5	59701,5	4,9
G2	5,8	51,3	5,2	11083,5	59701,5	5,4

A.5. Model for height as a function of time

Summarizing the intensity for the G-peak region (1540-1700) for each observation height, and plotting the height having the highest intensity for each measurement over time; yields the graph presented in *Figure 27*, according to the data in *Table A. 3*.

Table A. 3. Intensity over time for five observation heights recorded in model system during intercalation reaction.

t	0	2,5	5	7,5	10	t	0	2,5	5	7,5	10	t	0	2,5	5	7,5	10
180,141	278	226	113	62	20	705,625	-101	10	172	104	42	1266,25	-146	-127	-43	98	151
189,688	267	229	113	56	3	715,61	-109	-7	149	120	47	1277,06	-158	-126	-52	83	157
199,219	268	211	113	47	11	725,641	-114	2	152	133	47	1287,89	-155	-131	-55	82	157
208,735	282	198	110	51	-4	735,672	-115	-9	141	121	47	1298,7	-154	-127	-51	73	145
218,266	277	203	115	53	-2	745,719	-117	-10	145	123	46	1309,52	-154	-128	-70	61	159
227,75	270	206	96	49	13	755,781	-119	-28	133	119	44	1320,33	-158	-130	-56	64	148
237,281	276	191	100	57	13	765,828	-110	-28	132	128	54	1331,17	-155	-127	-62	67	157
246,797	261	229	124	62	9	775,891	-114	-33	121	120	52	1342,02	-150	-138	-76	59	167
256,344	269	230	119	68	19	785,969	-122	-29	123	112	48	1352,94	-146	-130	-70	44	170
265,906	252	242	112	50	18	796,078	-118	-37	107	132	64	1363,84	-152	-128	-78	37	161
275,469	259	236	132	54	18	806,203	-126	-43	114	137	44	1374,73	-152	-140	-84	35	167
285,047	253	253	113	63	15	816,328	-128	-39	105	145	54	1385,64	-158	-140	-85	29	169
294,61	231	260	116	73	23	826,453	-128	-43	101	132	66	1396,55	-160	-138	-94	18	164
304,172	242	255	132	65	15	836,594	-125	-44	104	133	68	1407,45	-146	-132	-93	19	157
313,75	245	263	126	58	28	846,719	-128	-56	89	141	55	1418,41	-157	-143	-95	13	159
323,328	241	264	135	75	19	856,985	-130	-54	99	153	67	1429,39	-159	-138	-93	5	139
332,985	255	283	135	72	27	867,266	-131	-55	86	146	66	1440,36	-153	-140	-94	2	157
342,625	234	258	153	78	36	877,531	-137	-59	83	153	62	1451,36	-160	-140	-97	0	145
352,266	258	356	170	101	36	887,797	-130	-64	80	143	67	1462,34	-150	-139	-99	-2	146
361,922	220	332	190	117	67	898,063	-136	-62	65	156	79	1473,33	-155	-153	-106	-4	129
371,563	227	404	231	147	91	908,328	-127	-64	79	152	65	1484,31	-160	-147	-109	-7	132
381,219	261	442	255	152	77	918,625	-129	-72	64	154	71	1495,36	-151	-151	-108	-16	122
390,891	239	437	257	155	100	928,985	-136	-75	70	160	82	1506,44	-159	-145	-103	-18	136
400,625	219	445	258	151	82	939,344	-148	-77	62	159	61	1517,52	-155	-151	-104	-20	129
410,344	180	380	226	126	79	949,703	-142	-77	61	156	79	1528,59	-156	-141	-109	-15	104
420,094	157	353	251	145	81	960,047	-125	-81	57	168	87	1539,66	-166	-145	-111	-29	112
429,813	100	284	208	108	68	970,406	-145	-75	41	155	75	1550,8	-156	-148	-119	-26	105
439,5	83	279	219	120	66	980,766	-139	-85	45	160	89	1561,95	-153	-151	-111	-33	107
449,188	59	252	198	110	53	991,156	-141	-85	51	156	74	1573,16	-157	-149	-111	-30	100
458,86	41	242	211	99	47	1001,578	-142	-79	29	172	99	1584,36	-154	-142	-113	-31	105

468,625	19	223	213	103	56	1012	-128	-100	26	167	100	1595,56	-165	-149	-116	-44	98
478,422	26	210	207	108	49	1022,453	-134	-85	24	158	97	1606,77	-156	-145	-125	-39	95
488,203	10	210	216	110	54	1032,891	-135	-97	28	151	91	1618	-163	-146	-123	-40	80
498	9	200	219	102	56	1043,344	-143	-94	22	155	110	1629,2	-159	-143	-117	-49	82
507,813	4	178	230	113	49	1053,781	-143	-95	25	159	98	1640,47	-158	-150	-121	-56	65
517,656	-4	192	223	119	65	1064,281	-134	-97	24	150	89	1651,75	-163	-154	-120	-73	68
527,547	-9	206	243	100	46	1074,781	-136	-101	5	152	105	1663,03	-157	-153	-126	-57	62
537,438	-27	173	237	113	69	1085,281	-141	-100	5	146	108	1674,31	-160	-151	-128	-63	46
547,344	-14	177	231	108	45	1095,797	-145	-101	5	135	108	1685,59	-156	-149	-135	-70	51
557,235	-40	140	237	113	55	1106,328	-138	-101	4	144	108	1696,89	-153	-149	-132	-72	47
567,063	-40	132	216	116	50	1116,844	-151	-115	-7	142	116	1708,19	-158	-149	-133	-72	48
576,875	-40	127	239	117	42	1127,391	-143	-109	-5	140	115	1719,56	-166	-152	-128	-75	39
586,625	-56	109	232	118	57	1137,969	-141	-110	-3	135	119	1730,94	-163	-155	-139	-81	32
596,36	-50	107	223	107	46	1148,563	-151	-105	-17	129	133	1742,31	-157	-154	-139	-84	23
606,235	-62	79	215	108	48	1159,156	-145	-116	-19	126	126	1753,67	-160	-156	-132	-90	27
616,125	-67	76	217	113	49	1169,781	-147	-114	-13	132	133	1765,05	-156	-154	-148	-85	20
626,016	-75	85	197	109	40	1180,39	-151	-115	-19	124	125	1776,44	-162	-155	-138	-94	18
635,922	-77	73	203	107	43	1191,08	-147	-120	-28	124	128	1787,83	-163	-157	-140	-85	3
645,813	-72	57	202	120	48	1201,77	-147	-110	-34	132	130	1799,27	-162	-159	-145	-89	9
655,781	-76	57	193	123	36	1212,5	-147	-126	-32	109	146	1810,72	-164	-152	-140	-98	8
665,75	-84	41	191	111	37	1223,25	-139	-123	-32	119	136	1822,17	-170	-150	-150	-106	0
675,703	-90	26	176	108	45	1234	-152	-125	-46	97	153	1833,64	-163	-158	-140	-101	-10
685,672	-97	20	166	104	48	1244,75	-148	-125	-53	106	154	1845,11	-159	-154	-140	-98	-13
695,656	-96	21	167	113	54	1255,48	-149	-129	-40	100	163	1856,56	-165	-155	-148	-106	-20
												1868,05	-166	-155	-149	-107	-27
												1879,58	-158	-164	-142	-110	-26
												1891,11	-155	-162	-145	-116	-42

A.6. Intensity shift model

By dividing the wavelength intensities for the stage-1 (1633 cm^{-1}) with the stage-2 signals (1621 cm^{-1}), over time. A relation between time and stage transition was established. The start of the data range selected was defined for when the stage-1 intensity was detected (>0) and the end of the data range was defined for when the stage-2 intensity was zero or negative. The values are presented below in *Table A. 4*.

Table A. 4. Intensities for 1632.91 cm-1 and 1621.3 cm-1 wavelength and the calculated relative intensity, for each observation height.

0 µm				2.5 µm				5 µm				7.5 µm				10 µm			
1633	1621	t	Rel. I	1633	1621	t	Rel. I	1633	1621	t	Rel. I	1633	1621	t	Rel. I	1633	1621	t	Rel. I
10	64	209	0,2	5	53	29	0,1	4	26	209	0,2	3	28	29	0,1	3	19	86	0,2
8	64	218	0,1	6	53	38	0,1	0	31	218	0,0	3	29	38	0,1	2	20	95	0,1
12	60	228	0,2	7	49	48	0,1	0	27	228	0,0	2	26	48	0,1	3	18	105	0,2
12	60	237	0,2	6	52	57	0,1	2	27	237	0,1	5	31	57	0,2	4	18	115	0,2
9	57	247	0,2	9	53	67	0,2	4	31	247	0,1	4	24	67	0,2	2	19	124	0,1
10	64	256	0,2	9	51	76	0,2	3	30	256	0,1	4	27	76	0,1	4	22	134	0,2
13	60	266	0,2	11	52	86	0,2	3	31	266	0,1	6	25	86	0,2	3	20	143	0,2
14	53	275	0,3	9	55	95	0,2	5	29	275	0,2	4	28	95	0,1	2	22	153	0,1
11	60	285	0,2	13	58	105	0,2	5	27	285	0,2	2	27	105	0,1	3	22	163	0,1
14	56	295	0,3	14	54	115	0,3	5	27	295	0,2	4	28	115	0,1	2	22	172	0,1
14	53	304	0,3	14	58	124	0,2	4	29	304	0,1	7	27	124	0,3	5	26	182	0,2
12	59	314	0,2	11	57	134	0,2	5	31	314	0,2	6	27	134	0,2	7	31	192	0,2
11	55	323	0,2	13	54	143	0,2	6	36	323	0,2	4	28	143	0,1	9	23	201	0,4
14	55	333	0,3	13	53	153	0,2	2	30	333	0,1	6	24	153	0,3	6	30	211	0,2
15	54	343	0,3	14	49	163	0,3	5	29	343	0,2	3	27	163	0,1	8	21	221	0,4
10	57	352	0,2	10	74	172	0,1	4	30	352	0,1	6	31	172	0,2	13	18	230	0,7
7	49	362	0,1	14	61	182	0,2	5	35	362	0,1	6	32	182	0,2	17	14	240	1,2
14	54	372	0,3	21	74	192	0,3	6	46	372	0,1	10	37	192	0,3	15	13	250	1,2
16	51	381	0,3	23	77	201	0,3	10	45	381	0,2	7	36	201	0,2	19	9	260	2,1
15	47	391	0,3	24	77	211	0,3	13	46	391	0,3	10	34	211	0,3	18	10	269	1,8
13	46	401	0,3	23	71	221	0,3	11	44	401	0,3	13	37	221	0,4	20	8	279	2,5
16	40	410	0,4	28	62	230	0,5	18	37	410	0,5	16	27	230	0,6	19	10	289	1,9
20	25	420	0,8	36	44	240	0,8	29	42	420	0,7	22	22	240	1,0	21	7	298	3,0
22	16	430	1,4	43	29	250	1,5	30	32	430	0,9	23	17	250	1,4	20	11	308	1,8
20	14	440	1,4	45	30	260	1,5	32	32	440	1,0	25	15	260	1,7	22	6	318	3,7
22	13	449	1,7	42	23	269	1,8	39	25	449	1,6	25	14	269	1,8	21	11	328	1,9
20	11	459	1,8	46	22	279	2,1	40	23	459	1,7	23	12	279	1,9	22	11	338	2,0
19	7	469	2,7	41	25	289	1,6	40	25	469	1,6	29	13	289	2,2	20	7	348	2,9
18	9	478	2,0	38	18	298	2,1	37	24	478	1,5	31	11	298	2,8	21	9	357	2,3
18	7	488	2,6	36	17	308	2,1	42	27	488	1,6	25	12	308	2,1	22	4	367	5,5
16	6	498	2,7	40	20	318	2,0	36	27	498	1,3	29	11	318	2,6	22	7	377	3,1
19	7	508	2,7	43	19	328	2,3	43	26	508	1,7	27	15	328	1,8	22	7	387	3,1
18	8	518	2,3	41	15	338	2,7	39	25	518	1,6	29	11	338	2,6	24	4	397	6,0
17	5	528	3,4	42	16	348	2,6	48	24	528	2,0	29	9	348	3,2	26	6	407	4,3
15	5	537	3,0	36	15	357	2,4	44	28	537	1,6	29	13	357	2,2	23	4	416	5,8

19	6	547	3,2	38	14	367	2,7	45	23	547	2,0	32	8	367	4,0	28	5	426	5,6
18	3	557	6,0	38	14	377	2,7	47	24	557	2,0	32	9	377	3,6	27	3	436	9,0
16	2	567	8,0	36	11	387	3,3	44	22	567	2,0	32	9	387	3,6	26	3	446	8,7
18	3	577	6,0	37	13	397	2,8	53	21	577	2,5	35	11	397	3,2	27	2	456	13,5
12	3	587	4,0	32	10	407	3,2	48	22	587	2,2	32	10	407	3,2	27	3	466	9,0
12	4	596	3,0	37	9	416	4,1	51	24	596	2,1	34	10	416	3,4				
				35	6	426	5,8	51	18	606	2,8	36	7	426	5,1				
				32	8	436	4,0	56	17	616	3,3	36	5	436	7,2				
				34	8	446	4,3	53	16	626	3,3	38	7	446	5,4				
				36	4	456	9,0	51	17	636	3,0	37	5	456	7,4				
				30	4	466	7,5	57	13	646	4,4	42	6	466	7,0				
				32	4	476	8,0	50	15	656	3,3	41	5	476	8,2				
								55	11	666	5,0	40	4	486	10,0				
								53	10	676	5,3								
								55	12	686	4,6								
								49	9	696	5,4								
								54	6	706	9,0								
								53	6	716	8,8								
								54	7	726	7,7								
								49	7	736	7,0								
								53	8	746	6,6								
								52	9	756	5,8								
								52	8	766	6,5								
								50	5	776	10,0								
								50	5	786	10,0								
								50	4	796	12,5								
								45	6	806	7,5								
								43	4	816	10,8								
								47	4	826	11,8								
								47	6	837	7,8								
								46	4	847	11,5								

A.7. SEM images of sulfuric acid expanded graphite

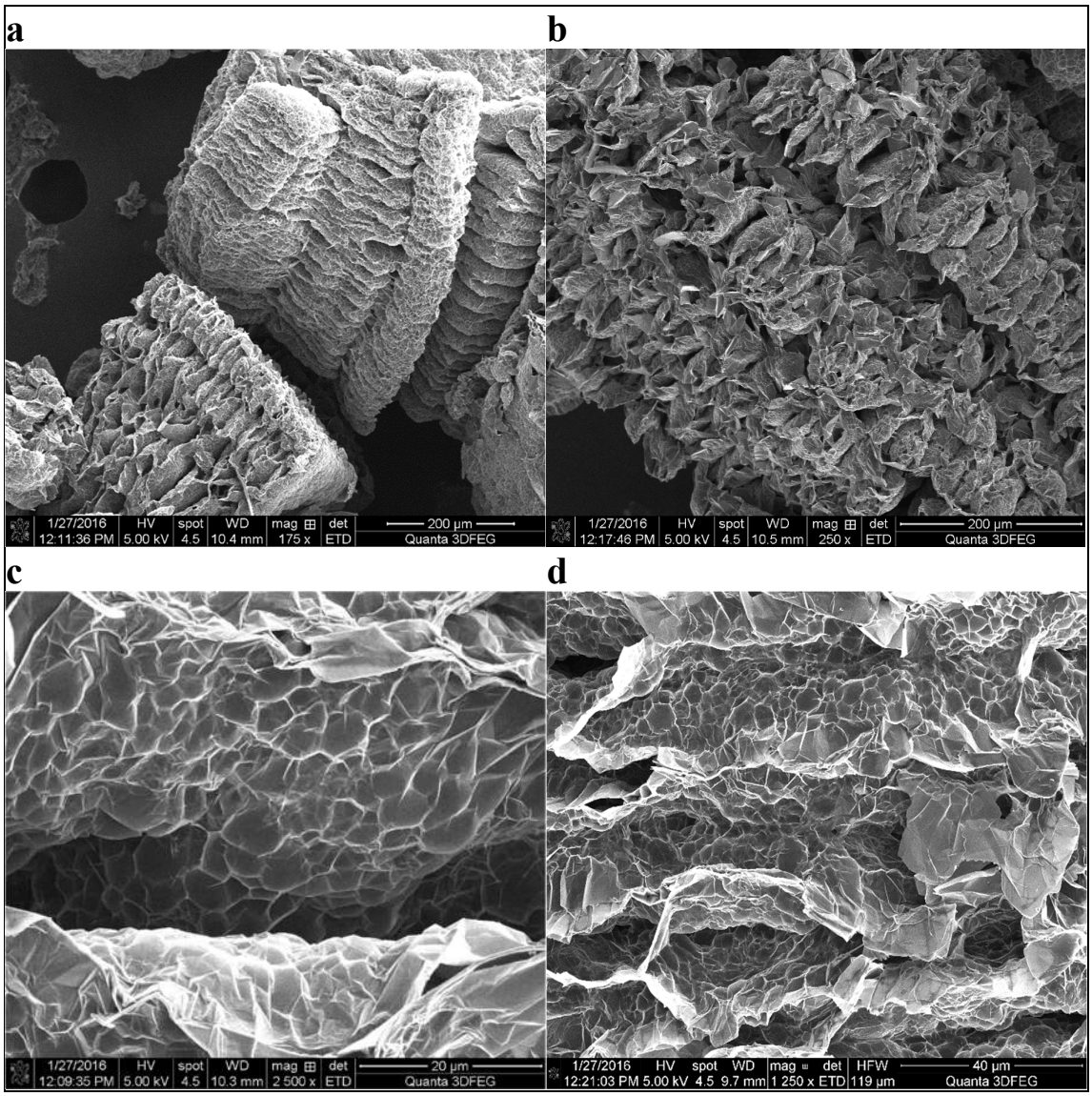

Figure A. 11 (a-d). SEM images acquired from the sulfuric acid expanded graphite described in *4.5 Acidic expanded graphite (page 28)*.

A.8. SEM images of microwave treated sulfuric acid expanded graphite

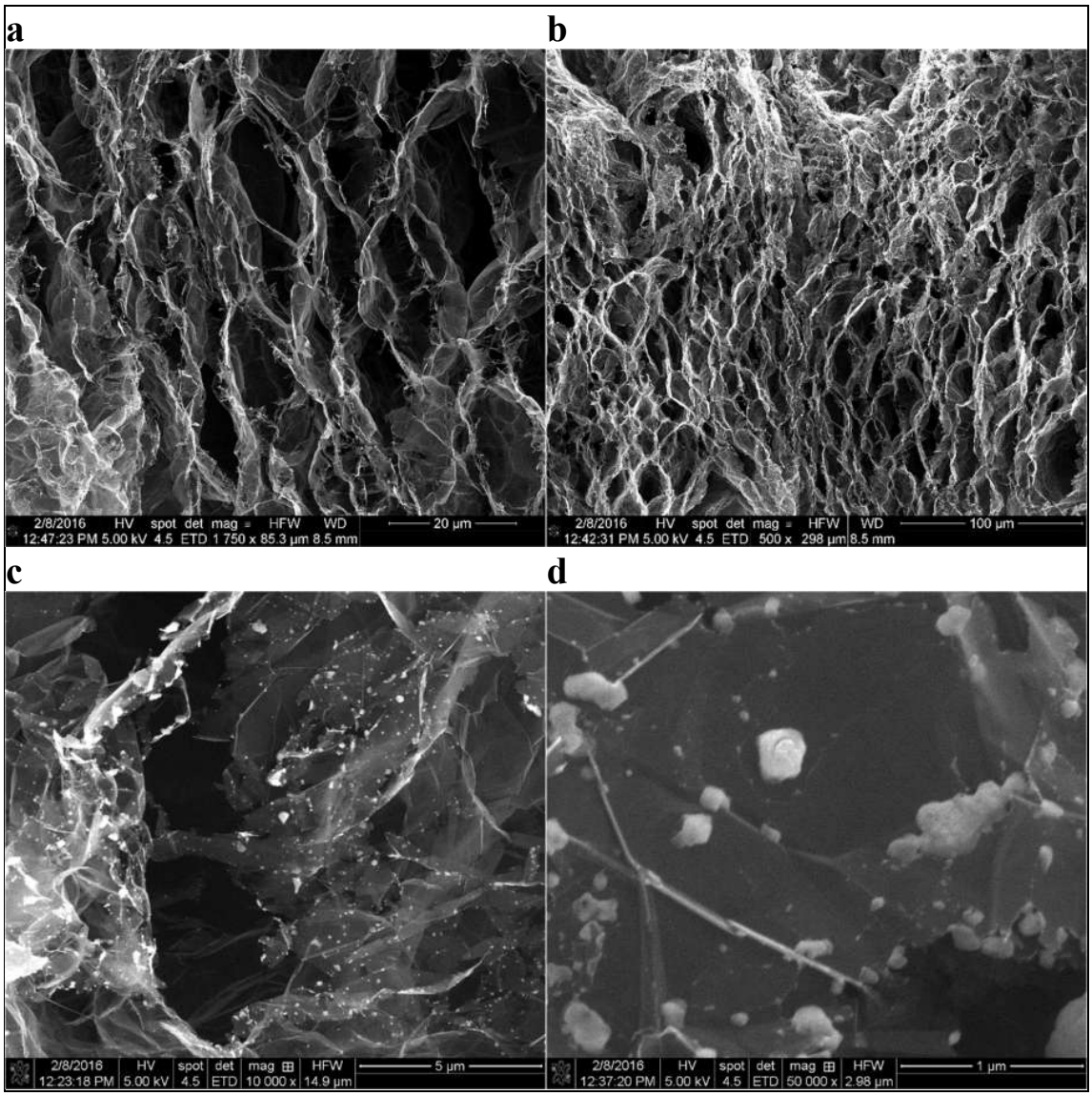

Figure A. 12 (a-d). SEM images acquired from the microwave treated sulfuric acid expanded graphite described in *4.5 Acidic expanded graphite (page 28)*.

A.9. Raman spectrum for sulfuric acid expanded graphite

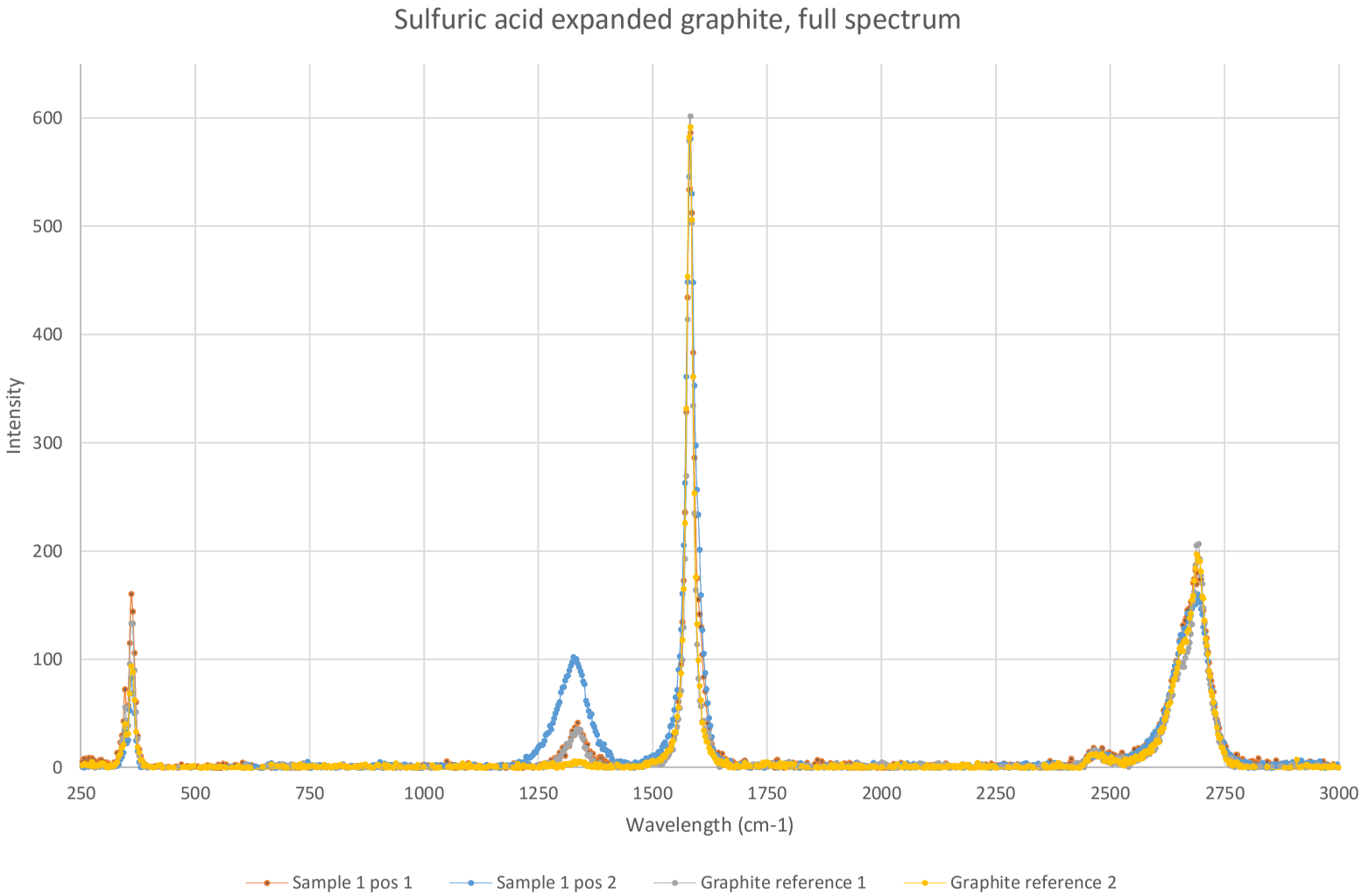

A.10. EDX analysis of sulfuric acid expanded graphite

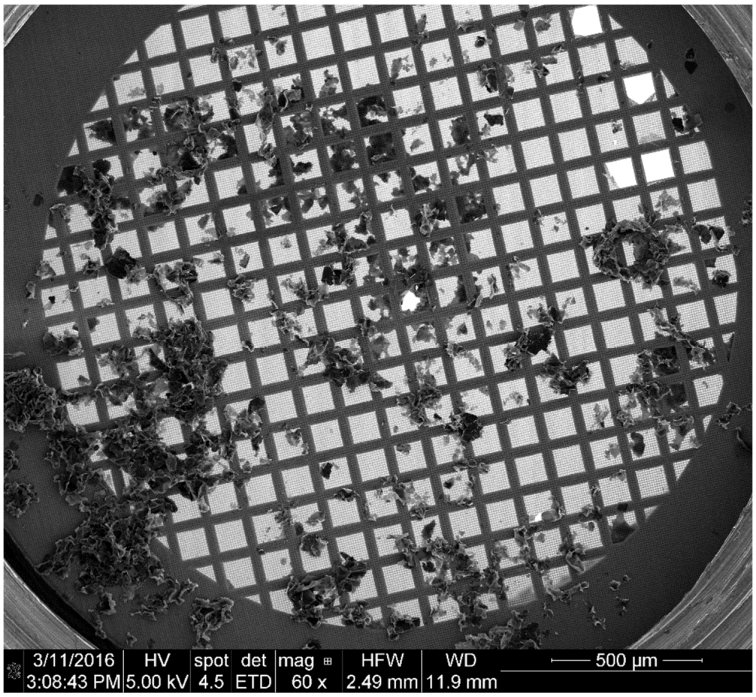

Figure A. 13. SEM image of the prepared TEM grid sample.

Table A. 5. Intstrument settings used for the linescan analysis data presented in *Figure 45*.

Line scan 1&2	
_Kv	5.0
_Mag	18123
_Tilt	0.0
_Detector	ADC1
_Averaging	16
_DataRange	0-4095
_Label	SE1
_Matrix	256x200
_MicronsPerPixX	0.051
_MicronsPerPixY	0.051